AD-A061 720 WAYNE STATE UNIV DETROIT MICH DEPT OF BIOLOGY F/G 6/1
CONTRIBUTIONS OF MEMBRANE COMPONENTS TO INTRACELLULAR WATER ORD--ETC(U)
NOV 78 P D MORSE N00014-76-C-1167

UNCLASSIFIED NL

1 OF 1
ADA
061720

END
DATE
FILMED
2-79
DDC

LEVEL II

No. 1
AO45450

Unclassified
SECURITY CLASSIFICATION OF [redacted]AGE (When Data Entered)

REPORT DOCUMENTATION PAGE

READ INSTRUCTIONS BEFORE COMPLETING FORM

1. REPORT NUMBER: Annual Report No. 2
2. GOVT ACCESSION NO.:
3. RECIPIENT'S CATALOG NUMBER:

4. TITLE (and Subtitle): Contributions of Membrane Components to Intracellular Water Order: Research on the Red Blood Cell and Spinach Thylakoid Membranes.

5. TYPE OF REPORT & PERIOD COVERED: Annual Report. no. 2, 1 Oct [redacted]77-Sep [redacted]978.

6. PERFORMING ORG. REPORT NUMBER:

7. AUTHOR(s): Philip D. Morse, II

8. CONTRACT OR GRANT NUMBER(s): N[redacted]14-76-C-1167

9. PERFORMING ORGANIZATION NAME AND ADDRESS:
Wayne State University
Department of Biology
Detroit, Michigan 48202

10. PROGRAM ELEMENT, PROJECT, TASK AREA & WORK UNIT NUMBERS: NR 207-011

11. CONTROLLING OFFICE NAME AND ADDRESS:
Office of Naval Research
Biophysics Program, 800 North Quincy Street
Arlington, Virginia 22217

12. REPORT DATE: 15 Nov [redacted]78

13. NUMBER OF PAGES: 63

14. MONITORING AGENCY NAME & ADDRESS (if different from Controlling Office):
Office of Naval Research Branch Office
536 South Clark Street
Chicago, Illinois 60605
64p.

15. SECURITY CLASS. (of this report): Unclassified

15a. DECLASSIFICATION/DOWNGRADING SCHEDULE:

16. DISTRIBUTION STATEMENT (of this Report)

Distribution of this document is unlimited.

17. DISTRIBUTION STATEMENT (of the abstract entered in Block 20, if different from Report)

18. SUPPLEMENTARY NOTES

19. KEY WORDS (Continue on reverse side if necessary and identify by block number)

Electron spin resonance, spin labels, membranes, red blood cells, spinach thylakoids, intracellular water order, diffusion, binding, membrane proteins.

20. ABSTRACT (Continue on reverse side if necessary and identify by block number)

This report describes the progress made in this laboratory during the year covered by the dates October 1, 1977 through September 30, 1978. The data and results presented here are continuations of work begun in the previous year (See Annual Report No. 1) and refinement of that work. Detailed descriptions of the measurements of the motion of the spin label TEMPAMINE (2,2,6,6-tetramethyl piperidine-N-oxyl-4-amine) in spinach thylakoids and red blood cells and ghosts are made. In addition, the possibility of the binding of this spin label to membrane proteins

DD FORM 1 JAN 73 1473 EDITION OF 1 NOV 65 IS OBSOLETE
S/N 0102-LF-014-6601

Unclassified
SECURITY CLASSIFICATION OF THIS PAGE (When Data Entered)

400 719

Block 20.

is dealt with. Our evidence shows that TEMPAMINE does not bind detectably to any membrane component or to hemoglobin. Thus, the motions associated with this spin label in the internal aqueous regions of cells arises from the interaction of the spin label with its immediate (micro) environment and is not due to artifactual binding of this label with membrane proteins. Materials and methods are described in detail.

OFFICE OF NAVAL RESEARCH

Contract N00014-76-C-1167

Task No. NR 207-011

ANNUAL REPORT NO. 2

"CONTRIBUTIONS OF MEMBRANE COMPONENTS TO INTRACELLULAR WATER ORDER: RESEARCH ON THE RED BLOOD CELL AND SPINACH THYLAKOID MEMBRANES"

by

Philip D. Morse, II

Wayne State University
Department of Biology
Detroit, Michigan 48202

15 November 1978

OFFICE OF NAVAL RESEARCH
BIOLOGICAL SCIENCES DIVISION
BIOPHYSICS PROGRAM, Code 444
DISTRIBUTION LIST FOR TECHNICAL, ANNUAL AND FINAL REPORTS

Number of Copies

(12) Administrator, Defense Documentation Center
Cameron Station
Alexandria, Virginia 22314

(6) Director, Naval Research Laboratory
Attention: Technical Information Division
Code 2627
Washington, D. C. 20375

(3) Office of Naval Research
Biophysics Program
Code 444
Arlington, Virginia 22217

(1) Commanding Officer
Naval Medical Research and Development Command
National Naval Medical Center
Bethesda, Maryland 20014

(1) Chief, Bureau of Medicine and Surgery
Department of the Navy
Washington, D. C. 20375

(2) Technical Reference Library
Naval Medical Research Institute
National Naval Medical Center
Bethesda, Maryland 20014

(1) Office of Naval Research Branch Office
495 Summer Street
Boston, Massachusetts 02210

(1) Office of Naval Research Branch Office
536 South Clark Street
Chicago, Illinois 60605

(1) Office of Naval Research Branch Office
1030 East Green Street
Pasadena, California 91106

(1) Commanding Officer
Naval Medical Research Unit No. 2
Box 14
APO San Francisco 96263

(1) Commanding Officer
Naval Medical Research Unit No. 3
FPO New York 09527

(1) Officer in Charge
Submarine Medical Research Laboratory
Naval Submarine Base, New London
Groton, Connecticut 06342

(1) Scientific Library
Naval Aerospace Medical Research Institute
Naval Aerospace Medical Center
Pensacola, Florida 32512

(1) Commanding Officer
Naval Air Development Center
Attn: Aerospace Medical Research Department
Warminster, Pennsylvania 18974

(1) DIRECTOR
Naval Biosciences Laboratory
Building 844
Naval Supply Center
Oakland, California 94625

(1) Commander, Army Research Office
P. O. Box 12211
Research Triangle Park
North Carolina 27709

(1) DIRECTORATE OF LIFE SCIENCES
Air Force Office of Scientific Research
Bolling Air Force Base
Washington, D. C. 20332

(1) Commanding General
Army Medical Research and Development Command
Forrestal Building
Washington, D. C. 20314

(1) Department of the Army
U. S. Army Science and
Technology Center - Far East
APO San Francisco 96328

(1) Assistant Chief for Technology
Office of Naval Research, Code 200
800 N. Quincy Street
Arlington, Virginia 22217

(1) ONR Resident Representative
University of Michigan
139 Cooley Building
2359 Bonisteel Blvd.
Ann Arbor, Michigan 48109

(1) Dr. Gilbert Ling
Pennsylvania Hospital
Department of Molecular Biology
8th and Spruce Streets
Philadelphia, Pennsylvania 19107

(1) Dr. Freeman W. Cope
Biochemistry Laboratory
U.S. Naval Air Development Center
Department of the Navy
Warminister, Pennsylvania 18974

(1) Dr. Carlton F. Hazlewood, Professor
Department of Pediatrics
Baylor College of Medicine
1200 Moursund
Houston, Texas 77030

ORIGINAL OBJECTIVES

1. How far does ordered water extend into the cell?
2. What are the contributions of the lipid and protein constituents of the membrane to water order?
3. Does the water inside a cell represent a different state of water compared to bulk water?

The purpose of this report is to outline the progress made toward these objectives during the year Oct. 1977 through Sept. 1978.

STUDIES UNDERTAKEN DURING THE CONTRACT YEAR 1977-1978

During the first year of this contract, I made several fundamental investigations of the motion of the spin label TEMPAMINE (2,2,6,6-tetramethyl-piperidine-N-oxyl-4-amine) in the aqueous interior of red blood cells, red blood cell ghosts, and spinach thylakoids (see First Annual Report). The motion of a spin label is related to the viscosity of the medium it samples. (See First Annual Report and Appendix I). However, in complex biological systems, other factors that can affect spin label motion can come into play. Because the spin label TEMPAMINE is a charged entity, it is a likely candidate for binding to charged groups on membrane surfaces and on protein molecules. The question then arises "How is spin label (TEMPAMINE) motion in a complex biological system related to internal viscosity?". We have approached this problem in a number of different ways. The first was to simply perform calculations to determine the distance over which a spin label could diffuse during the time it was conveying information about its local environment. The second was to study long term and short term binding of TEMPAMINE to intact membranes, disrupted membrane components, and non-membrane proteins such as hemoglobin. The third was to determine if TEMPAMINE was asymmetrically distributed within the lumen of any cell

membrane bound system. Since these efforts occupied the whole of the

problems mentioned, and our resolution of them where possible.

SHORT AND LONG TERM BINDING OF TEMPAMINE TO AND ITS DISTRIBUTION IN RED BLOOD CELLS, RED BLOOD CELL GHOSTS, HEMOGLOBIN, INTACT CHLOROPLASTS, AND DISRUPTED CHLOROPLASTS

Binding of TEMPAMINE to red blood cell components

TEMPAMINE which is bound to some intracellular or membrane component may alter the distribution of TEMPAMINE such that the spin label would be accumulated inside the cells. This possibility was studied by incubating intact red blood cells, unsealed ghosts membranes, and resealed ghosts in 1 mM TEMPAMINE for one hour followed by rapid centrifugation and immediate analysis of the supernatant by ESR. Whole cells were used to determine the binding of TEMPAMINE to the hemoglobin as it is arranged inside the cell while leaky ghosts were used to study TEMPAMINE binding to the membrane alone. The resealed membrane preparations were used to eliminate the possibility of non-specific accumulation of TEMPAMINE by ion gradients across the cell membrane in the intact or resealed cells.

The results of these experiments are shown in Table I. The concentration of TEMPAMINE in the suspension of cells was taken as unit value and the concentration of TEMPAMINE in the supernatant was compared to this. The pellets could not be examined directly because they were too viscous to sample. If TEMPAMINE was bound to either intracellular hemoglobin or to the membrane, then there would be less TEMPAMINE in the supernatant than in an equivalent volume of the total cell suspension. The results in Table I show that, within error, there is no difference in the concentration of TEMPAMINE in the suspensions and supernatants of the red blood cells, the unsealed ghosts, or the resealed ghosts.

The above experiment demonstrates equal distribution of TEMPAMINE between the cells and the external solution, but it is still possible that TEMPAMINE is asymmetrically distributed inside the red cells or resealed ghosts. This would

again be caused by spin label which is bound either to hemoglobin or to the membrane. Regional distribution could also give regions of increased spin label concentration such that collisions between spin labels would be more frequent and exchange broadening would result (1,2). This increases the line width of the 1 mM TEMPAMINE signal beyond the line width expected from motional considerations alone.

The results with red blood cells, resealed cells and hemoglobin are shown in Table II. The expected line widths are measured from spectra of 1 mM TEMPAMINE in glycerol-water mixtures of 5 centipoise for the red cells and 2 centipoise for the resealed ghosts. Line width data is normalized in this manner because line width is dependent on spin label motion, which is in turn dependent upon viscosity (1). The mid field line was chosen for these measurements since it is least affected by variations in spin label motion (3). The average mid field line width of TEMPAMINE inside the red blood cells was 1.57 ± 0.07 gauss and may be compared to 1.60 gauss for TEMPAMINE in a glycerol-water mixture with a bulk viscosity of 5 centipoise. The mid field line width obtained from resealed ghosts was 1.63 ± 0.12 gauss and may be compared to 1.54 gauss for a glycerol-water mixture with a bulk viscosity of 2 centipoise. Because there is no statistical difference between line widths of TEMPAMINE in the cells and in glycerol-water, these results suggest that TEMPAMINE is randomly distributed inside the red cells and resealed ghosts.

Since both hemoglobin and TEMPAMINE are charged at pH 7.5, additional experiments were performed to further check for binding between TEMPAMINE and hemoglobin (Table II). The mid field line width of 1 mM TEMPAMINE in a solution of 3% hemoglobin was 1.53 ± 0.01 gauss. The rotational correlation time of TEMPAMINE in 3% hemoglobin shows that this solution has a microviscosity of 1.2 centipoise. A glycerol-water mixture of the same microviscosity gives a mid field line width of 1.53 gauss. A 12% hemoglobin solution has a

microviscosity of 3.1 centipoise and the mid field line width was 1.53 ± 0.01 gauss. A corresponding glycerol-water mixture has a mid field line width of 1.54 gauss. The fact that these line widths are equal within error suggests that TEMPAMINE is randomly distributed in these hemoglobin solutions. This, in conjunction with the line width data from the intact cells, suggests that the spin label is not bound to hemoglobin in the red blood cell.

Strong binding between TEMPAMINE and hemoglobin may be further examined by an analysis of the spectral line shapes. The spectra did not show any immobilized component. However, binding between TEMPAMINE and hemoglobin may still occur as a rapid equilibrium during the lifetime of the excited state of TEMPAMINE (10^{-8} sec. ref.1). Evidence of equilibrium binding may be detected by changes in the rotational correlation time of TEMPAMINE in 27% hemoglobin as a function of TEMPAMINE concentration. Assuming rapid equilibrium between free and bound TEMPAMINE, such as: $\text{TEMPAMINE} + \text{hemoglobin} \overset{\text{fast}}{\rightleftharpoons} \text{TEMPAMINE-hemoglobin}$, then higher ratios of TEMPAMINE to hemoglobin should shift the equilibrium away from the formation of hemoglobin-TEMPAMINE complexes. The unbound TEMPAMINE would then give rise to a decrease in the apparent rotational correlation time of TEMPAMINE. Similarly, lower ratios should increase the apparent rotational correlations times of TEMPAMINE.

The data presented in Table III corresponds to hemoglobin:TEMPAMINE ratios ranging from about 500:1 to 5:3. There is no change in τ_c over the range of TEMPAMINE concentrations studied. This suggests that the equilibrium binding between TEMPAMINE and hemoglobin molecules lies far to the left and hence no binding is observed.

We conclude from the above studies that the results presented in Table IV are an actual reflection of the intracellular viscosity and are not caused by binding of the spin labels either to the membrane or to hemoglobin.

Binding of TEMPAMINE to spinach thylakoids

Binding or other factors which may cause an unequal distribution of TEMPAMINE in the thylakoids will alter the motion of TEMPAMINE such that τ_c would be modified. For this reason, the degree of interaction between TEMPAMINE and the thylakoid components was determined before studying the motion of TEMPAMINE in the aqueous interior of the thylakoids. Both intact thylakoids and thylakoids sonicated in 20% Triton X-100 were studied. The sonicated thylakoids were totally disrupted so that TEMPAMINE would have an opportunity to interact with previously unexposed sites on and within the thylakoid membrane.

In the first experiment, τ_c was measured in a very concentrated suspension of intact thylakoids (20-30 mg chlorophyll/ml) and in thylakoids disrupted by Triton X-100. TEMPAMINE motion is expected to decrease in both cases because of the high bulk viscosity of the thylakoid suspension. The data from this experiment is shown in Table V. The rotational correlation time of TEMPAMINE in water at 25 C is used as a reference point to compare the rotational motion of TEMPAMINE in the intact and dispersed thylakoids. In a sample of packed intact thylakoids, τ_c increased by a factor of 1.9 relative to τ_c in bulk water while τ_c in the Triton dispersed thylakoid preparation increased by a factor of 2.6 relative to water and 1.2 relative to a control solution of 20% Triton X-100. The spectra obtained from both thylakoid preparations showed no immobilized spin label component which suggests that TEMPAMINE is not irrotationally bound. Nevertheless, some rapid equilibrium binding could account for the increase in τ_c in the thylakoid samples, especially since TEMPAMINE is a charged species at pH 7.5 and there are probably charged groups on the thylakoid membrane which could interact with TEMPAMINE. This could appear as an accumulation of TEMPAMINE by the thylakoids even in the absence of strong binding.

The second experimental series was designed to measure long and short term accumulation of TEMPAMINE by the thylakoids and is summarized in Table VI. First, intact and sonicated thylakoids were dialized against 10 volumes of 5 mM TEMPAMINE

for 48 hours. Some reduction of TEMPAMINE was noted but this did not affect the calculations since we noted that the reduced spin label also equilibrated between dialysate and the external solution. Table VIA shows that the concentration of TEMPAMINE was greater in the dialysate than in the external solution for the intact thylakoids, but not for the sonicated thylakoids. Thus, some accumulation of TEMPAMINE by intact thylakoids does occur over a long period of time.

TEMPAMINE binding which may occur in the time frame of the ESR measurements was studied by centrifuging untreated thylakoids (25,000 g for 15 minutes) in normal washing buffer containing 5 mM TEMPAMINE and comparing the concentration of TEMPAMINE in the supernatant with the concentration in the suspension. Table VIB shows that the concentrations of TEMPAMINE in the suspension and supernatant were equal within error after the 15 minute centrifugation. This shows that measurable binding of TEMPAMINE does not occur during the time that the ESR experiments are performed.

In summary, the results from the experiments described in this section show that any interactions between TEMPAMINE and the thylakoid components will not hinder the rotational motion of TEMPAMINE by a factor of greater than 2.

MOVEMENT OF TEMPAMINE DURING HYPERFINE LIFETIME

Factors restricting the motion of TEMPAMINE in intact red blood cells

A number of mechanisms could account for our results. One is that TEMPAMINE binds to hemoglobin during some part of its excited state which seems unlikely as discussed previously. Perhaps TEMPAMINE diffusion and hence TEMPAMINE motion is restricted in some way by the presence of hemoglobin, or the environment sampled by TEMPAMINE is actually more viscous than bulk water.

Water inside an intact red blood cell is never very far away from hemoglobin. If hemoglobin is taken to be a cylinder 57 Å in diameter with a center to center distance of 95 Å at 5 mM (4) which is the approximate concentration of hemoglobin in the red blood cell under isoosmotic conditions, then there is a

38 Å channel of water between hemoglobin molecules. Over the range of 200 to 500 mOsm, the range we studied, this distance can vary about 25%. Perutz determined that there should be a layer of water one molecule thick around each hemoglobin (5) although this has been questioned by Gary-Bobo and Solomon (6). Thus the aqueous environment inside the intact red blood cell is characterized by water in close association with hemoglobin. Since TEMPAMINE can sample bound water (7) then TEMPAMINE would be expected to give information about the average microviscosity of the cell interior. Considering the lifetime of the excited state of TEMPAMINE, estimated at 10^{-8} sec. , TEMPAMINE would move about 35 Å in a medium with a bulk viscosity of 5 centipoise. Changes in the relative amounts of "free" and "bound" water as a function of osmolarity and pH (6) could thus easily account for the variation in relative immobility of TEMPAMINE in the red cell interior.

It is also possible that the water channels in packed hemoglobin would restrict the diffusion of TEMPAMINE. Keith et al (2) have shown that the spin label 2,2,6,6-tetramethyl piperidine-N-oxyl-4-one shows restricted motion in the channels formed by the beads used for gel filtration. Smaller pore diameters restricted spin label motion more than did larger pore diameters. Thus, swelling and shrinking the red blood cells by osmotic mechanisms would cause a change in this pore size and result in a change of TEMPAMINE motion. In the absence of information about the "state" of water in these pores, it is difficult to assign these changes in spin label motion to more frequent collisions between the spin labels and the "walls" of the channel, or to an increased quantity of "bound" water inside the channels. We cannot at present make statements concerning the state of water inside the intact red blood cell on the basis of our results.

Factors restricting the motion of TEMPAMINE in resealed red blood cell ghosts

Interpretation of results with resealed ghosts is actually less complex.

Ghosts prepared by our methods are about 80-90% as large as intact cells and still retain their bi-concave shape (8,9). Since TEMPAMINE is randomly distributed within the lumen of these cells, the average TEMPAMINE molecule is 2000 Å - 5000 Å away from any surface at any given time. To our knowledge, no soluble proteins exist within these resealed cells although it is remotely possible that some of the inward-facing proteins such as spectrin could be released during the resealing process and trapped inside the cell. Electron microscopic evidence, however, shows no osmium staining material in the cell lumen after resealing (9).

For rapid binding between TEMPAMINE and the proteins of the cell membrane to give the observed results, TEMPAMINE would have to be bound 1/2.5 of the life time of the excited state. If we take 10^{-8} sec as the excited state lifetime, we calculate that all the TEMPAMINE would have to be within 76 Å of the membrane to interact this way. This distance is insufficient to explain the distribution of spin labels within the ghost in this manner. Furthermore, entropy considerations would dictate that some TEMPAMINE be present in the center of the lumen where it would tumble with a rotational correlation time equivalent to that of bulk water. Again, this is not observed by us. We are therefore forced to conclude that the aqueous interior of the ghost is more viscous than bulk water but the mechanism by which this could occur is unclear. We are presently performing experiments to illucidate the role of membrane proteins and lipids on the intracellular viscosity of the resealed ghosts.

Factors restricting the motion of TEMPAMINE in spinach thylakoid preparations

The rotational correlation time is a measure of the tumbling rate of a spin label, such that any restriction of tumbling by binding may be reflected as an increase in correlation time. However, on the basis of our results, we conclude that binding of TEMPAMINE by the thylakoids cannot entirely explain the restricted

motion of TEMPAMINE in the thylakoid lumen. We have three reasons for this conclusion.

First, there was no evidence of TEMPAMINE immobilization in the spectra. This rules out irrotational binding of TEMPAMINE by the thylakoid suspension. Second, there was no short term accumulation of TEMPAMINE molecules by the intact thylakoid dialysate, but this can be explained by a gradual movement in response to a small pH gradient which might exist across the membrane. This inward flux of TEMPAMINE appears to be so gradual, however, that it is not significant within the time frame of our experiments.

The above experiments do not rule the possibility that the restricted motion of TEMPAMINE in the intrathylakoid space may result from very rapid interaction between TEMPAMINE and the thylakoids (10, 11). It is theoretically impossible to determine if the observed increase in τ_c is due to TEMPAMINE tumbling in a medium which reduces isotropic motion by a factor of ten, or if TEMPAMINE is free to rotate only 1/10 of the time. However, the following practical considerations may help in deciding which of these two possibilities is the best interpretation of our data.

Interaction between TEMPAMINE and the thylakoid membrane which may occur during the lifetime of the excited state of the spin label (10^{-8} sec, ref. 1) requires that TEMPAMINE be within a certain distance from the thylakoid membrane. This distance can be calculated as follows. The Stokes equations for viscosity and diffusion may be combined to obtain $D = 0.22\ r^2/\tau_c$, where D is the diffusion coefficient and r is the radius of the diffusing molecule (1). The one-dimensional diffusion distance is calculated from the equation $X = \sqrt{2DT}$ where X is the distance in cm and T is the time in seconds. For TEMPAMINE in a 1 centipoise solution, where r = 3 Å and $T = 10^{-8}$ sec, X is 50 Å. If we take into account the observation that TEMPAMINE motion is restricted (by whatever mechanism) by a factor of 10, X is reduced to 10 Å. This means that in order to account for our results in terms of TEMPAMINE-membrane interactions, only those

TEMPAMINE molecules located within 10 Å of the membrane may interact with the membrane at any given time. If TEMPAMINE is randomly distributed in the thylakoid lumen, then only 20% of the intrathylakoid TEMPAMINE is available for interaction with the membrane since the thylakoid interior under the conditions of this study is 100 Å across. If we further assume that the intrathylakoid space is similar to bulk water, then the remaining 60% of the TEMPAMINE would yield an ESR signal characteristic of TEMPAMINE in bulk water (see Fig. 1A). The total signal from the thylakoid under these conditions would consist of a small, broadened signal from the TEMPAMINE close to the membrane and a large, sharp signal from the TEMPAMINE in the thylakoid lumen. The signal height of the broadened signal would be greatly reduced compared to the sharp signal due to the relationship between line height and line width (W^2h = constant). Thus, the sharp signal would predominate in the ESR signal arising from the thylakoid interior and it is from this signal that correlation time and microviscosity are calculated. Therefore, since TEMPAMINE interaction with the thylakoid membrane is a very small contributor to the total ESR intrathylakoid signal, and since the signal we observe is characteristic of TEMPAMINE tumbling in a solution with a microviscosity of 10 centipoise, then we may conclude that the intrathylakoid environment is much more viscous than bulk water.

The above analysis relies on random distribution of TEMPAMINE in the thylakoid lumen. TEMPAMINE-membrane interaction would strongly influence τ_c only if most of the TEMPAMINE was located within 10 Å of the membrane. In this case, however, the TEMPAMINE concentration would appear to increase by about a factor of 5, which would induce an increase in line width from spin-spin interactions (1,12-16). . At a bulk viscosity of 10 centipoise, 25 mM TEMPAMINE has a mid field line width of 2.15 gauss. All values of the mid field line widths in the thylakoid suspensions are well below this (Figure 1C and 1E, see figure legend). This strengthens our assumption that most of the TEMPAMINE is randomly distributed within the thylakoid interior.

Finally, the rotational correlation time of TEMPAMINE is slowed within the spinach thylakoids only if the membrane is intact. Total disruption by Triton sonication yields a mixture that is not as effective in restricting the motion of TEMPAMINE as are intact preparations of thylakoids. One possible interpretation of this result is that the intact membrane provides a surface which leads to the ordering of water. This has been demonstrated by Keith, Snipes, and Chapman for artificial phospholipid complexes (7). An additional aspect of their study is that spin labels, including TEMPAMINE, will partition into ordered water and are not excluded by it. The fact that the rotational correlation time of TEMPAMINE is increased by a factor of ten in the thylakoid lumen certainly does not demonstrate the existance of ordered water inside thylakoids, however, it is one possible interpretation that is consistent with our results.

CONCLUSIONS

The data and discussions presented above lead to several conclusions about the motion and distribution of TEMPAMINE within the lumen of cells or organelles. These are:

1) TEMPAMINE motion is related to the viscosity of the environment (as expected). Thus, if TEMPAMINE were present in an intracellular environment with a relatively low viscosity and a relatively small intramembrane distance (say, a spinach thylakoid 100 Å across with an internal viscosity of 2 centipoise) would be able to interact with the cell membrane. These two interacting elements, viscosity, and intramembrane distance, must be tightly controlled in order to perform experiments with spin labels in which there is a minimum uncertainty about interaction of the spin label with the cell membrane.

2) TEMPAMINE does not interact detectably with any known membrane components or proteins (such as hemoglobin) over the concentration ranges studied. Thus, even if the opportunity for TEMPAMINE-membrane interaction arose, its

probability of occuring is low. I believe that this is due to the fact that TEMPAMINE is primarily protonated at the pH values used in these studies, but that a considerable number of other cations are also present which would compete for charged sites with TEMPAMINE. This minimizes TEMPAMINE interaction with membrane charged sites.

3) Given the above considerations, it seems most probable that TEMPAMINE is indeed reporting the microviscosity of the interior of cells and organelles under the conditions we employ. Thus, the thylakoid interior seems to have a viscosity about 10-fold greater than bulk water, while intact red blood cells have a viscosity about 5 times greater, and resealed ghosts about 2.5 times greater than bulk water. At present, we do not know the source of these increased viscosities. We are currently studying the contributions of red blood cell membrane proteins and lipids toward this phenomena.

METHODS

The following sections describes the methodology employed in our laboratory to study the internal viscosity of cells and organelles.

Preparation of resealed red blood cell ghosts

Inorganic chemicals were obtained from Mallinckrodt (AR grade) and organic chemicals were obtained from Sigma. Water was twice distilled in glass. Antibody-positive ACD whole blood was obtained from the Detroit Red Cross and used well before the expiration date. No attempt was made to select blood according to ABO or Rh antigens. Particulate matter and cell aggregates in the whole blood were removed with a nylon mesh filter. Protein and hemoglobin concentrations were assayed by the methods of Lowry et al. (17) and Drabkin and Austin (18), respectively. Hematocrits were determined after a 10 minute centrifugation on an Adams Autocrit™ Centrifuge.

Preparation of Ghosts

The procedure we followed to prepare ghosts was essentially that of Steck (19). All operations were performed at 4°C. Fifteen mls of whole blood were washed 3 times with 25 mls of 150 mM NaCl-5 mM sodium phosphate buffer, pH 8.0 (phosphate-buffered saline, PBS) and sedimented at 6000 g for 10 minutes with a JA-20 rotor in a Beckman J-21B centrifuge. The supernatant and buffy coat were carefully removed by aspiration after each wash. The washed cells were lysed with a 30-fold excess of 5 mM phosphate buffer, pH 8.0 (5P8), and the ghosts were immediately sedimented at 27,500 g for 10 minutes. The supernatant was aspirated and care was taken to remove the cellular debris and unlysed cells which form a tight button beneath the lysed red cells. The lysis procedure was carried out 3-4 times to remove all traces of hemoglobin. After the final sedimentation, the concentration of ghost protein in the pellet was 3 mg/ml compared to standards of bovine serum albumin (see Table VII).

Preparation of Resealed Ghosts

A 10-fold excess of PBS was added to the white ghosts and the suspension was incubated for 1 hour at 37 C. The partially sealed ghosts were then immediately centrifuged at 27,500 g for 10 minutes at 4 C without the use of the centrifuge brake. The supernatant was removed, and the pellet of ghosts stored overnight at 4°C to complete the resealing process.

Assays for Resealing

Glyceraldehyde-3-phosphate dehydrogenase (GaPDH) activity was assayed by the method of Steck and Kant (20). As a control, 0.2% Triton X-100 was added to release GaPDH activity hidden by cell resealing. Resealing was also assayed by electron spin resonance (ESR) following the method of Morse (21). In this method, 91 µl of ghosts were placed in a 10 x 75 test tube along with 1 µl of 100 mM TEMPAMINE (2,2,6,6-tetramethylpiperidine-

N-oxyl-4-amine) and 8 μl of 1 M $K_3Fe(CN)_6$. The sample was then drawn up into a 1 mm I.D. glass capillary, heat-sealed, placed inside a 3 mm I.D. quartz ESR tube, and inserted into the ESR cavity. ESR spectra were measured on a Varian E-109 E spectrometer at the following settings: modulation amplitude of 0.5 gauss, power at 5 milliwatts, 4 minute time scan, and a time constant of 0.128 seconds. The spectrometer was equipped with an E-238 TM cavity. All spectra were recorded at room temperature ($25^{\circ} \pm 3^{\circ}C$). Integrated signal intensity was calculated from the equation: $A = W^2h$/instrument gain, where A is the area, W is the peak to peak width of a first derivative ESR line, and h is the height of that line (22).

Light Microscopy

The resealed vesicles with and without trapped hemoglobin as well as samples from each of the 4 lyses were prepared for light microscopy in the following manner. The samples were diluted 1:1 with PBS and were placed on acid-cleaned microscope slides between two parallel glass rods. The glass rods were used as bases for the cover slips so as not to crush the samples. Photographs were taken on a Leitz Orthoplan-Orthomat light microscope under Smith T interference optics with oil immersion at 2250X.

Electron Microscopy

Resealed and unsealed ghosts were prepared for electron microscopy in the following manner. The samples were fixed in 2% glutaraldehyde, 0.2 M sucrose and 0.1 M cacodylate buffer, pH 7.4, for 1 hour at 4 C. This mixture was hypertonic to the cells and some deformation in shape was expected. The fixed membranes were washed 3 times in 0.2 M sucrose and 0.1 M cacodylate buffer, pH 7.4, and then post-fixed in 1% osmium, 0.2 M sucrose and 0.1 M cacodylate buffer, pH 7.3, for 1 hour at 4 C. After post-fixation, the membranes were again washed as above. Dehydration was performed by a graded series of ethanol-water mixtures (50-100%)

followed by exchange into propylene oxide. The cells were then embedded in Epon and heated at 37°C, 45°C, and 60°C for 24 hours at each temperature. The blocks were sectioned on a Sorvall Porter-Blum MT-2 ultra-microtome and post-stained in 0.5% uranyl acetate followed by 0.5% lead citrate. The sections were imaged with a Philips 201 electron microscope.

Analysis of Resealing by GaPDH and ESR

The membrane bound enzyme GaPDH is found on the interior of the erythrocyte membrane (19). Resealing of the membrane makes the substrate unavailable to the enzyme and this results in a decrease of enzyme activity. GaPDH was assayed at 10 minute intervals during incubation of the ghosts at 37°C (Figure 2). During the hour that the cells were exposed to this temperature, GaPDH activity fell to approximately 20% of the Triton control levels. This indicates that at least one of the components of the enzyme assay was not available to the enzyme.

The ESR resealing assay (Figure 2) relies on the ability of potassium ferricyanide to broaden the signal of TEMPAMINE when the two molecules are close enough for this interaction to occur (21, 23). If a situation exists where TEMPAMINE can partition into a space where ferricyanide is not present, then only the TEMPAMINE signal will be detectable at low instrument gains. In unsealed ghosts, both TEMPAMINE and ferricyanide will equilibrate throughout the cell suspension. After the ghosts have resealed, ferricyanide added to the cell suspension cannot enter the internal aqueous compartment, while TEMPAMINE can easily cross the membrane (21) into the cell interior. The TEMPAMINE signal which is detected under these conditions is characteristic of a spin label tumbling rapidly in an aqueous environment. This free, aqueous spin label signal, indicative of membrane resealing, was not observed when the ghosts were assayed during or after 1 hour of heating at 37°C. Only after overnight incubation at 4°C did this signal appear.

Determination of Yield of Resealed Ghosts

The integrated intensity of the TEMPAMINE signal in red blood cells in the presence of potassium ferricyanide is proportional to the hematocrit of the cells (21). Thus, the ESR spectrum provides an estimate of the volume of cells which excludes ferricyanide. Assuming that resealed ghosts at a concentration of 3 mg membrane protein per ml are packed to about the same density as intact red blood cells at a hematocrit of 100%, the percentage of ghosts resealing to ferricyanide can be calculated. For example, a sample of 1 mM TEMPAMINE, intact red blood cells at a hematocrit of 100%, and 80 mM potassium ferricyanide gave a signal intensity of 4.48 arbitrary units. A similar sample containing resealed ghosts instead of intact cells gave an intensity of 2.24 units. It follows that 2.24/4.48 x 100 = 50, or 50% of the ghosts have resealed. Typical resealing values were in the range of 10-50%.

Effects of Variations in the Resealing Procedure

Each step in the resealing process was varied in order to determine the effect on the ability of the cells to reseal to ferricyanide. 1) The age of the blood was very important. Resealing would not occur if the blood was near or past its expiration date. 2) It was necessary to filter the blood through nylon mesh to remove any particulate matter. This matter contaminated the cells during the lysis procedure and prevented resealing. 3) Deviations of more than 0.5 pH units or 2°C during washing, lysis, or incubation would also prevent resealing. Other factors which prevented resealing were incubation at 37°C for longer than 1 hour, exposure of the heat-treated cells to room temperature for any period prior to centrifugation at 4°C, and centrifugation of the heat-treated cells at forces greater than 27,000 g or longer than 10 minutes. The procedure described in the METHODS section optimizes the yield of sealed ghosts.

Morphology of Lysed Cells and Resealed Ghosts

The cells and ghosts were examined by light microscopy (Figure 3) and electron microscopy (Figure 4). The light micrographs show during the lysis steps (3A-D) the ghosts are shaped as spheres and stomatocytes, but after resealing (3E), the ghosts are mainly echinocytes and biconcave discs. The resealed ghosts which contain trapped hemoglobin (3F) appear to be in much better condition than those ghosts which were resealed in PBS alone. Very few echinocytes are present and there is a larger percentage of the normal biconcave disc shape. The electron micrographs (Figure 4) show that the membrane morphology is not noticeably altered by the lysis steps or the resealing procedure. The processes of fixing and embedding for electron microscopy cause distortions in cell shape, but fine structural detail is nevertheless revealed by these micrographs, such as the dense material seen inside the cells in 4F.

Gel electrophoresis of the cells during lysis and resealing is shown in Figure 5. Sample numbers 1 through 4 represent the total number of lysis steps to which the cells were subjected. There is no detectable loss in any of the membrane proteins during lysis. However, the amount of hemoglobin associated with the cells is reduced considerably. The resealed ghosts are shown in sample 5. When compared to the ghosts from which they were prepared (sample 4), there is also no detectable change in the banding pattern of the membrane proteins.

Preparation of spinach thylakoids for experiments to measure internal viscosity and binding

All thylakoid preparations were carried out at $4^{o}C$. Class II chloroplasts (thylakoids, without outer membranes) were isolated from deveined spinach leaves (Spinacea oleracea). The leaves were homogenized in a solution containing 300 mM NaCl, 30 mM Tricine-NaOH (pH 7.7), and 3 mM $MgCl_2$. The resulting suspension was filtered through eight layers of Miracloth and centrifuged (2500 g for 3 minutes),

The pellet of thylakoids was resuspended in a solution containing 200 mM sucrose, 20 mM Tricine-NaOH (pH 7.5), and 3 mM $MgCl_2$, centrifuged (2500 g for 5 minutes), resuspended in the same sucrose medium containing an additional 0.1 mg/ml bovine serum albumin and centrifuged again (2500 g for 5 minutes). The final thylakoid pellet was loosened with a small paintbrush and used without dilution in the ESR experiments.

Some modifications of the thylakoid preparation were made for the spin label binding studies. For those experiments in which the thylakoids were treated with Triton X-100, the leaves were homogenized as above except that the buffer did not contain $MgCl_2$. The $MgCl_2$ was omitted to facilitate disruption of the membranes. After filtration, the thylakoids were washed two times in a solution of 100 mM sucrose and 10 mM Tricine-NaOH (pH 7.5), and centrifuged (48,000 g for 10 minutes). The final thylakoid pellet was mixed one to one with 40% Triton X-100 (v/v) and sonicated at 30% of full power with an Artek Sonic 300 Dismembranator. The preparation was examined by light microscopy and no intact thylakoids were observed.

For dialysis, 1 ml of thylakoids was placed in dialysis tubing (10 mm wide) and suspended in 10 ml of the corresponding final washing buffer containing 5 mM TEMPAMINE. The samples were stirred slowly at 4°C for 48 hours. During dialysis, some reduction of the TEMPAMINE by the thylakoids was noted. Further reduction after dialysis was avoided by mixing 1 volume of the thylakoids with 10 volumes of chloroform:methanol (2:1).

The initial chlorophyll concentrations in the various thylakoid preparations were about 8 mg chlorophyll/ml when determined by the method of Arnon (11). For some of the ESR experiments it was necessary to pack the thylakoids in hematocrit tubes which increased the concentrations to 20-30 mg chlorophyll/ml. The tubes were centrifuged (10,000 g for 10 minutes) in an Adams Autocrit Centrifuge.

Sample preparation for ESR studies

Red Blood Cells

ESR spectra were recorded with a Varian E-109 E spectrometer at the following settings: modulation amplitude at 0.5 gauss; power at 5 milliwatts; scan times, 2 to 4 minutes; and time constants on 0.128 to 0.5 second. The spectrometer was equipped with an E-238 TM cavity and an E-257 temperature controller.

The ESR experiments described in this paper were of two types. The first type examined the rotation of a water-soluble spin label, TEMPAMINE, in the intracellular compartment of the red blood cell or resealed ghost. Potassium ferricyanide (Mallinckrodt) was used to broaden the TEMPAMINE signal not associated with the internal space. This method is described in full detail in reference 21 and the First Annual Report.

The ESR samples containing the water-soluble spin label, TEMPAMINE, were prepared as follows: 1 μl of 100 mM TEMPAMINE in water was placed in the bottom of a 10 x 75 mm test tube and 99 μl of the red cell or resealed ghost suspension containing up to 80 mM $K_3Fe(CN)_6$ were added. All samples were then mixed and drawn up into a 1 mm I.D. glass capillary, flame-sealed, and placed inside a 3 mm I.D. quartz tube before insertion in the ESR cavity. Temperatures of the samples in the cavity were controlled by a nitrogen gas flow system and monitored with a copper-constantan thermocouple placed against the sample in the quartz tube. Temperature fluctuations at a single point were less than 0.05 C, but there was a large temperature gradient (about 2°C) along the sample. Care was used to ensure that the thermocouple was measuring temperature at the active region of the sample, that is, where the ESR signal was being measured. This distance was about 1 cm along the length of the sample, and the variation in temperature over this distance was on the average of $\pm$ 0.5°C.

Rotational correlation times (τ_c) were calculated using the approximations described by Keith et al. (3, see Appendix I) which yield the equation:

$$\tau_c = kW_o \left\{ (h_o/h_{-1})^{\frac{1}{2}} - 1 \right\}$$

where k is a constant which depends on the values of the g and hyperfine tensors for the spin label and the microwave frequency. The other parameters, W_o, h_o, and h_{-1}, are the first derivative peak to peak mid field line width, mid field line height, and high field line height, respectively. The integrated intensity was calculated from the equation: $A_o = W_o^2 h_o$/instrument gain, where A is the area under the first derivative line.

The internal microviscosity reported by TEMPAMINE inside the red cells or resealed ghosts was obtained by comparisons of the rotational correlation time of TEMPAMINE in water to that of TEMPAMINE in the samples.

Spinach thylakoids

Electron spin resonance (ESR) spectra were measured on a Varian E109-E spectrometer with a gas flow temperature regulator. Measurements with a copper-constantan thermocouple showed that the temperature at any given point along the sample varied only $\pm$ 0.1°C, but a vertical temperature gradient of about 2°C/cm existed along the long axis of the sample. Temperatures reported in this paper were measured with the sample and thermocouple at the geometric center of the cavity, thus ensuring that the recorded temperature accurately corresponded to the region of the sample from which the ESR spectrum was recorded.

Rotational correlation times (τ_c) were calculated from the equation (3, see Appendix I) :

$$\tau_c = kW_o \left\{ \left(\frac{h_o}{h_{-1}} \right)^{\frac{1}{2}} - 1 \right\}$$

where k is a constant which depends on the principal values of the g and hyperfine tensors for the spin label and on the microwave frequency. The other parameters,

W_o, h_o, and h_{-1} are the first derivative peak to peak mid field line width, mid field line height, and high field line height, respectively. For the purpose of this paper, the major limitation of this formula is that it requires isotropic tumbling of the nitroxide spin label.

The ESR samples were prepared as follows: 87 μl of the thylakoid suspension and 5 μl of 100 mM TEMPAMINE were placed in the bottom of a 10 x 75 mm test tube and mixed thoroughly. Then, 8 μl of 1 M $K_3Fe(CN)_6$ (Malinckrodt) were added. The suspension was mixed again, drawn up into a 1 mm I.D. glass capillary and carefully heat sealed. The capillary was placed inside a 3 mm I.D. quartz tube along with the temperature probe and the ESR spectrum was recorded. Typically, the preparation of the ESR sample was completed in less than one minute.

The modulation amplitude was kept below 1/3 of the narrowest line width, or 0.5 gauss, whichever was smaller. The microwave power was 5 milliwatts. No microwave saturation was noted at this power setting. Scan times ranges between 0.5 and 4 minutes.

USE OF THE DESCRIPTIVE TERM "INTERNAL MICROVISCOSITY"

The problems associated with the term internal microviscosity have been discussed. (1, 23) In general, viscosity measurements using spin labels require that the solvent be uniform and isotropic and that no interactions occur between the solvent and the spin label. In certain cases, we can only assume that these requirements are satisfied, and because of this we use a comparative analysis of viscosity and define the term η_μ where η_μ is obtained from the ratio of the rotational correlation time of TEMPAMINE in the cell to the rotational correlation time of TEMPAMINE in water at 25°C (4×10^{-11} sec), $\eta_\mu = \tau_c$ (cell)/ τ_c (water). This is a relative measurement and does not give absolute values of the viscosity inside the cell. In addition, any given TEMPAMINE molecule can only sample a small region inside the cell. Although spin label rotation is related to bulk viscosity in a linear manner (1), the spin label only provides

information about a microenvironment and hence only yields data about microviscosity. However, the relative microviscosities obtained from this technique will reliably indicate increases or decreases in η under variable experimental conditions.

PUBLICATIONS DURING THE REPORTING PERIOD

Morse, Philip D., (1977). Localization of the membrane perturber adamantyl sulfate in sarcoplasmic reticular vesicles. Chemistry and Physics of Lipids: 20, 295-303.

Berg, Steven P. , Lusczakoski, D. , and Morse, Philip D., II. (1979). Spin label motion in the internal aqueous compartment of spinach thylakoids. Archives of Biochemistry and Biophysics (accepted for publication)

MANUSCRIPTS IN PREPARATION

Lusczakoski, D. , Simpson, D. A. , and Morse, Philip D., II. The internal microviscosity of red blood cells and hemoglobin-free ghosts: A spin label study.

Simpson, D. , Lusczakoski, D. , Mizukami, H. , Palazzo, R. , Menter, D. , Johnson, R. M. , and Morse, Philip D., II. Preparation of hemoglobin-free resealed red blood cell ghosts and entrapment of exogenous hemoglobin.

REFERENCES

1. Morse, P.D., II, Ruhlig, M., Snipes, W., and Keith, A.D. (1975) Arch. Biochem. Biophys. 168:40-56.

2. Keith, A.D., Snipes, W., Mehlhorn, R.J., and Gunter, T. (1977) Biophys. J. 19:205-218.

3. Keith, A., Bulfield, G., and Snipes, W. (1970) Biophys. J. 10:618-629.

4. Riley, D.P. and Heubeut D. (1950) Biochem. Biophys. Acta 4:37.

5. Perutz, M.F. (1928) Science 201:1187-1191.

6. Gary-Bobo, C.M. and Solomon, A.K. (1968) Journal of Gen. Physiol. 52: 825-853.

7. Keith, A.D. , Snipes, W., and Chapman, D. (1977) Biochemistry 16, 634-641.

8. Morse, P.D., II, Simpson, D., Mizukami, H., Lusczakoski, D., and Palazzo, R. (1968) J. Supramol. Structure 8 (supplement 2) p.206

9. Simpson, D., Lusczakoski, D., Mizukami, H., Johnson, R., Palazzo, R., Mentor, D., and Morse, P.D., II (1978) submitted for publication.

10. Finch, E.D. and Harmon, R.A. (1974) Science 186, 157-158.

11. Snipes, W. and Keith, A.D. (1974) Science 186, 158.

12. Jost, P. and Griffith, O.H. (1976) in "Spin Labeling Theory and Applications", L.J. Berliner, ed. Academic Press, New York, pps. 251-273.

13. Plachy, W. and Kivelson, D. (1967) J. Chem. Phys. 47, 3312-3318.

14. Eastman, W., Bruno, G.V., and Freed, J.H. (1970) J. Chem. Phys. 52, 2511-2522.

15. Salikhov, K.M., Doctorov, A.B., Molin, Y.N., and Zamaraev, K.I. (1971) J. Magn. Resonance 5, 189-205.

16. Deveaux, P., Scandella, C.J., and McConnell, H. (1973) J. Magn. Resonance 9, 474-485.

17. Lowry, O.H., Rosebrough, H.J., Fahr, L., and Randall, R.S. (1951) J. Biol. Chem. 193:265-275.

18. Drabkin, D.L. and Austin, J.H. (1932) J. Biol. Chem. 98:719-733.

19. Steck, T.L. (1974) in "Methods in Membrane Biology, Vol. II", E.D. Korn, ed., Plenum Press, New York - London, pps. 245-281.

20. Steck, T.L. and Kant, J.A. (1975) in "Methods in Enzymology, Vol. 31", S. Fleischer and L. Packer, eds., Academic Press, New York, pps. 172-180.

21. Morse, P.D., II (1977) Biochem. Biophys. Res. Comm. 77:1486-1491.

22. Snipes, W. and Keith, A. (1970) Res. Dev. Feb.:22-26.

23. Berg, S.P., Lusczakoski, D., and Morse, P.D., II, Arch. Bioc. Biop. in press.

TABLE AND FIGURE LEGENDS

Table I. Measurement of TEMPAMINE accumulation by red blood cell, resealed ghosts, and unsealed ghosts. TEMPAMINE (1 mM) was added to a preparation of cells, resealed ghost, or unsealed ghosts, and incubated at room temperature for one hour. The samples were then centrifuged at 40,000 g for 10 minutes (5,000 g for 10 minutes for the intact cells), and the supernatant collected. The supernatant was then compared with samples taken from the original mixture of cells and buffer and their relative signal intensities were compared. The values obtained from the suspensions were arbitrarily set to 100% and the supernatants compared to that. Each entry in the table is the average of two experiments. Within error, there is no difference in the concentrations of TEMPAMINE between the supernatant and the suspensions in all three cases.

Table II. Spectral line widths of TEMPAMINE in red blood cells, resealed ghosts, and hemoglobin. Rotational correlation times were first obtained from the samples and glycerol-water mixtures were prepared of identical viscosities. The line widths of TEMPAMINE in these solutions are shown in the last column. When these line width values are compared with those obtained from the samples listed in the first column, it can be seen that there is no significant difference between the values obtained in the red cell sample, the ghost sample, or the hemoglobin samples, and those obtained for the glycerol-water solutions of identical viscosity.

Table III. Rotational correlation time of TEMPAMINE at various TEMPAMINE-hemoglobin ratios. Over a range of 1:500 to 3:5, there is little difference in τ_c. This indicates that TEMPAMINE does not bind to hemoglobin.

Table IV. Average values of microviscosity for red blood cells and hemoglobin-free resealed ghosts. These values were obtained from 15 to 20 samples under the standard conditions of 320 mOsm, pH 7.5, and 25°C. Microviscosity is calculated from the ratio of the rotational correlation time of TEMPAMINE in the sample to that in water at 25°C.

Table V. Measurement of τ_c in intact and disrupted thylakoids. The column on the right is the ratio of τ_c of TEMPAMINE in the sample to τ_c of TEMPAMINE in the corresponding reference medium such that the degree to which TEMPAMINE motion is hindered in each sample may be compared. Water is used as the reference in the upper portion of the table while 20% Triton X-100 is used as the reference in the lower portion.

Table VI. Accumulation of TEMPAMINE by thylakoids. Each entry in the table represents an average of three separate experiments. A. Samples were dialysed for 48 hours against 5 mM TEMPAMINE. The concentration of TEMPAMINE in the external solution was taken as unit value and the concentrations in the corresponding dialysate was normalized accordingly. B. Intact thylakoids in 5 mM TEMPAMINE were centrifuged for 15 minutes and the concentration of TEMPAMINE in the supernatant was compared to its concentration in the suspension. The pellets could not be directly examined because they were extremely viscous and could not be easily drawn into the hematocrit tubes. Since speed of sampling was important, only the supernatants were used. Thylakoids which were Triton-treated produced no pellets upon centrifugation.

Table VII. The concentration of hemoglobin in washed and lysed red blood cells. Red cells were washed 3 times in PBS and then lysed 4 times in 5P8 as described in the METHODS section. The total protein and hemoglobin concentrations were measured after the final wash and after each lysis step.

The column on the right is the percentage of the total protein which can be attributed to hemoglobin. Typically, the amount of hemoglobin remaining after the fourth lysis was less than 0.4% of the total protein. This represents a dilution of the original hemoglobin by 26,000.

LEGENDS

FIGURE 1. ESR spectra of control and thylakoid samples. The hyperfine coupling constant is 16.9 gauss.

A. 5 mM TEMPAMINE alone in water. The flat line is 5 mM TEMPAMINE and 80 mM potassium ferricyanide at the same instrument gain as the spectrum of TEMPAMINE alone (8×10^1).

B. 5 mM TEMPAMINE and 80 mM potassium ferricyanide at an instrument gain of 3.2×10^3. The spectrum becomes much broader but τ_c does not change.

C. Suspension of thylakoids containing 5 mM TEMPAMINE and 80 mM potassium ferricyanide. The hyperfine coupling constant is 16.4 gauss which compares favorably with that of TEMPAMINE in water, and the midfield line width is 1.93 gauss. An average microviscosity calculated from 10 spectra is 11.15 ± 0.85. This suspension was centrifuged and the pellet and supernatant separated for further ESR studies (see D and E).

D. Supernatant from 3C which contains ferricyanide and TEMPAMINE external to the thylakoids. Note the similarity of this spectrum to that shown in 3B. Spectrometer gain setting as in 3C.

E. Signal obtained by digitally subtracting spectrum 3D from spectrum 3C. The hyperfine coupling constant of this spectrum is 16.7 gauss and the midfield line width is about 2.00 gauss. The average microviscosity of five separate subtractions is 10.18 ± 0.41. This spectra is characteristic of TEMPAMINE tumbling in a medium with a viscosity of 10 centipoise (see 3F).

F. 5 mM TEMPAMINE in glycerol-water with a bulk viscosity of 10 centipoise. The hyperfine coupling constant is 16.5 gauss and the midfield line width is 1.70 gauss.

FIGURE 2. Resealing of white ghosts to glyceraldehyde-3-phosphate dehydrogenase (GaPDH). The cells were first assayed for GaPDH activity by the method of Steck (5), and then an identical control sample was run in the presence of Triton X-100 to determine the intrinsic GaPDH rate which was used as the 100% level. Over the course of 1 hour, 80% of the cells sealed to GaPDH.

FIGURE 3. Light micrographs of ghosts in various stages of lysis and resealing. Bars are equivalent to 10 microns. A) After first lysis step; B) After second lysis step; C) After third lysis step; D) After fourth lysis step; E) After resealing in PBS; and F) After resealing in hemoglobin-PBS solution. The cells containing hemoglobin (F) have a biconcave shape, although not as pronounced as the intact red blood cell.

FIGURE 4. Electron micrographs of ghosts in various stages of lysis and resealing. Bars are equivalent to 1 micron. A)-F), as in Figure 3. The stained material noted in 4F is hemoglobin.

FIGURE 5. Gel electrophoresis of ghosts in various stages of lysis and resealing. Gel electrophoresis followed the method of Fairbanks et al. (12) on a 4-12% acrylamide gradient. Columns 1 through 4 represent 25 μl samples from lysis steps 1 through 4, respectively. Column 5 represents a 25 μl sample of resealed ghosts. The banding pattern of the proteins does not change for any of the samples, with the exception of the loss of hemoglobin during the lysis steps.

TABLE I

Sample	Suspension	Supernatant
unsealed ghosts	100	98.1 ± 2.0
resealed ghosts	100	99.3 ± 0.7
red blood cells	100	98.7 ± 6.2

taken from two runs.

TABLE II

Sample	W_o	Corresponding η	W_o
red blood cells	1.57 ± 0.08	5.5 cP	1.60
resealed ghosts	1.63 ± 0.12	2.3 cP	1.54
12% hemoglobin	1.53 ± 0.01	3.1 cP	1.54
3% hemoglobin	1.53 ± 0.01	1.2 cP	1.53

TABLE III

(TEMPAMINE) mM	τ_c in 27% Hb
.01	1.21×10^{-10}
.03	1.09×10^{-10}
.1	1.18×10^{-10}
.3	1.14×10^{-10}
1.0	1.13×10^{-10}
3.0	1.21×10^{-10}

TABLE IV

AVERAGES VALUES OF MICROVISCOSITY OF RED BLOOD CELLS AND HEMOGLOBIN-FREE RESEALED GHOSTS

Red Blood Cells	5.47 ± 2.04
Resealed Ghosts	2.34 ± 0.42

TABLE V

MEASUREMENT OF γ_c IN INTACT AND DISRUPTED THYLAKOIDS

5 mM TEMPAMINE samples (at 25°C)	γ_c	$\frac{\gamma_c(\text{sample})}{\gamma_c(\text{reference})}$
Water	4.0×10^{-11}	1.0
Untreated Thylakoids	7.6×10^{-11}	1.9
Thylakoid dispersion in 20% Triton X-100	10.4×10^{-11}	2.6
20% Triton X-100 alone	8.8×10^{-11}	1.0
Thylakoid dispersion in 20% Triton X-100	10.4×10^{-11}	1.2

TABLE VI

ACCUMULATION OF TEMPAMINE BY THYLAKOIDS

		External solution	Dialysate (thylakoids)
A.	Untreated **	1.00 ± 0.28	1.77 ± 0.23
	Triton sonicated*	1.00 ± 0.02	0.94 ± 0.18
B.			
	Untreated*	1.00 ± 0.26	0.91 ± 0.21

* No significant difference at the 99% level

** Significant differences at the 99% level

TABLE V II

HEMOGLOBIN REMAINING IN WASHED RED BLOOD CELLS AND GHOSTS

Number of lyses	Total protein	Total hemoglobin	$\frac{\text{Total hemoglobin}}{\text{Total protein}} \times 100$
0	319 ± 25	320 ± 48	100
1	30.5 ± 3.28	26.4 ± 0.13	86 ± 8.8
2	4.97 ± 0.71	1.53 ± 0.26	31 ± 8.4
3	3.08 ± 0.14	0.136 ± 0.030	4.4 ± 1.1
4	3.21 ± 0.17	0.0123 ± 0.0008	0.36 ± 0.04

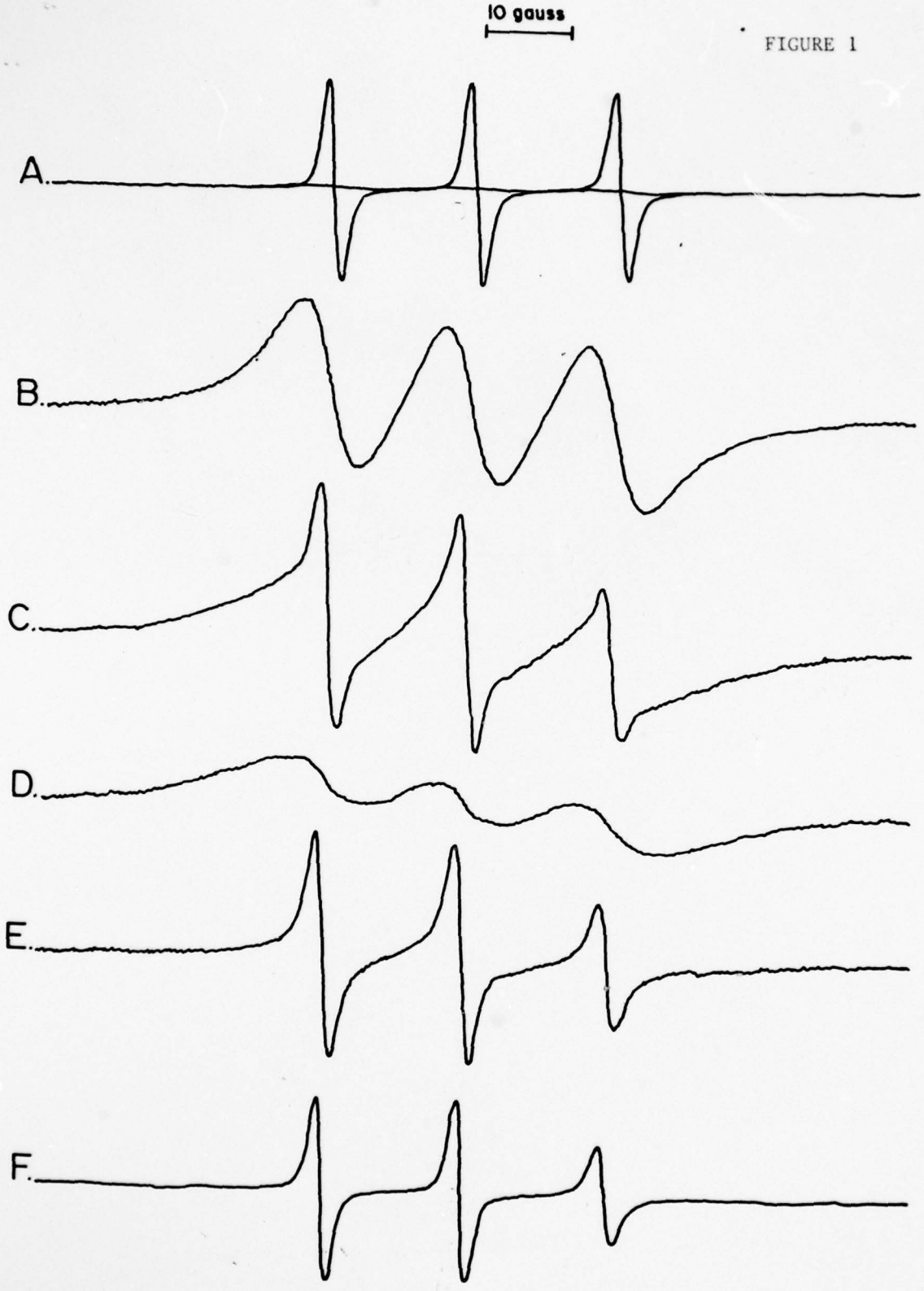

FIGURE 1

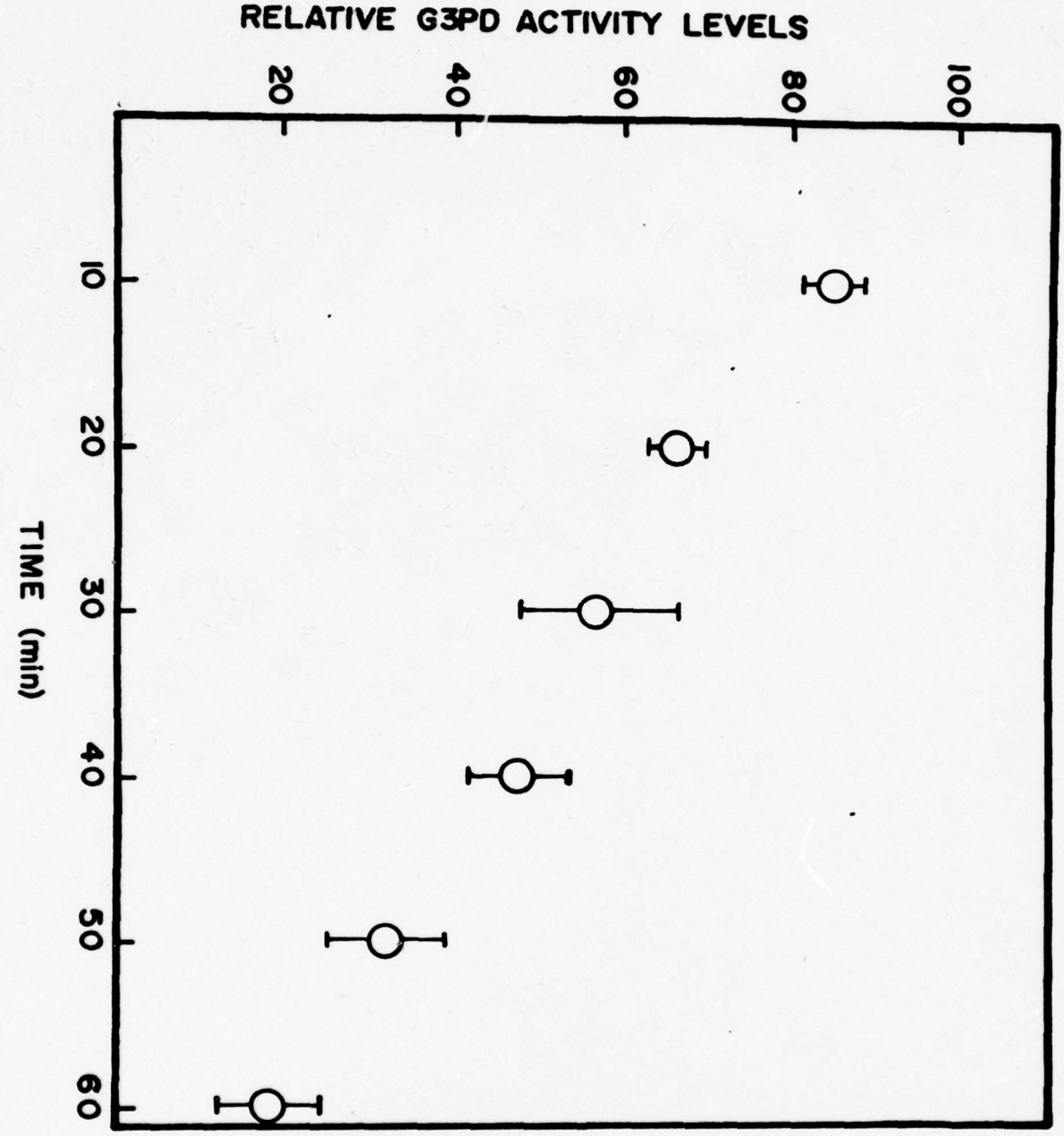
RELATIVE G3PD ACTIVITY LEVELS
20
40
60
80
100
TIME (min)
10
20
30
40
50
60

FIGURE 2

FIGURE 3

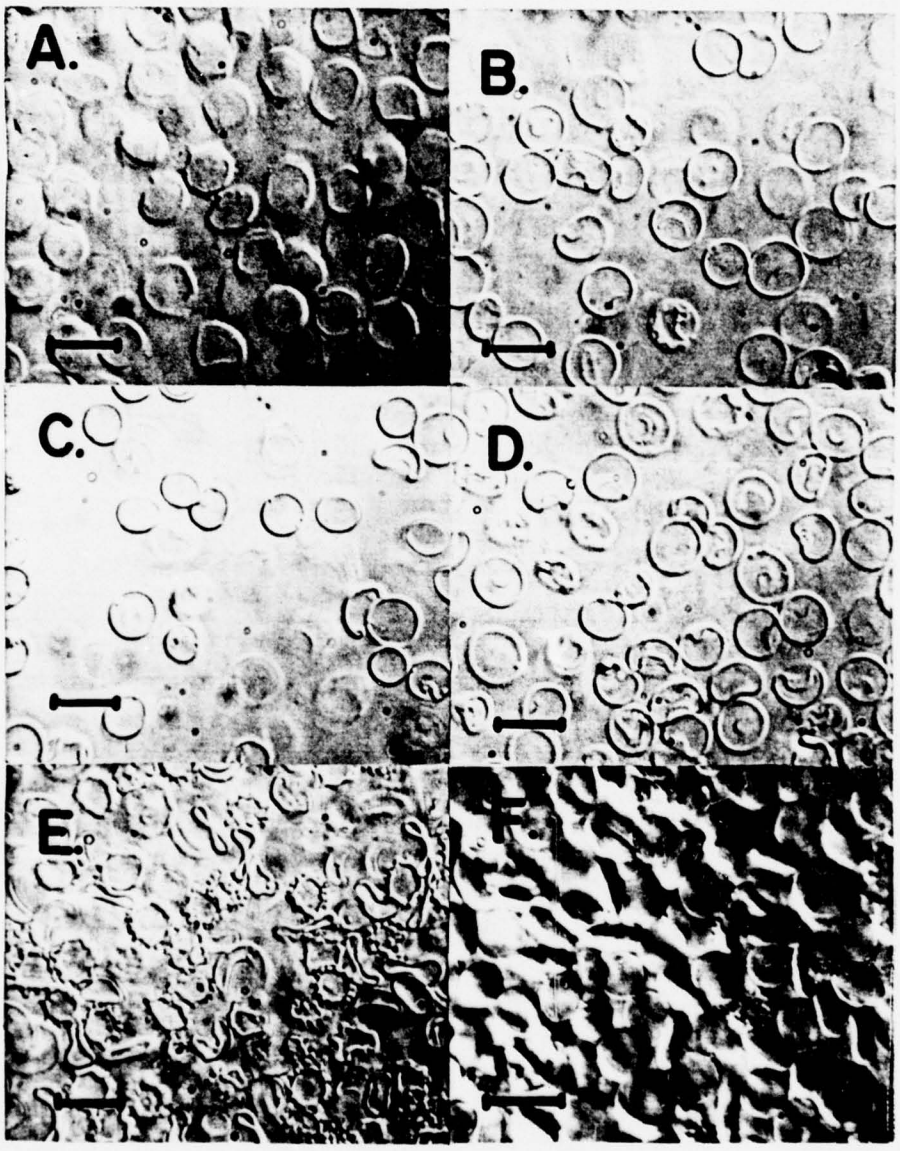

FIGURE 4

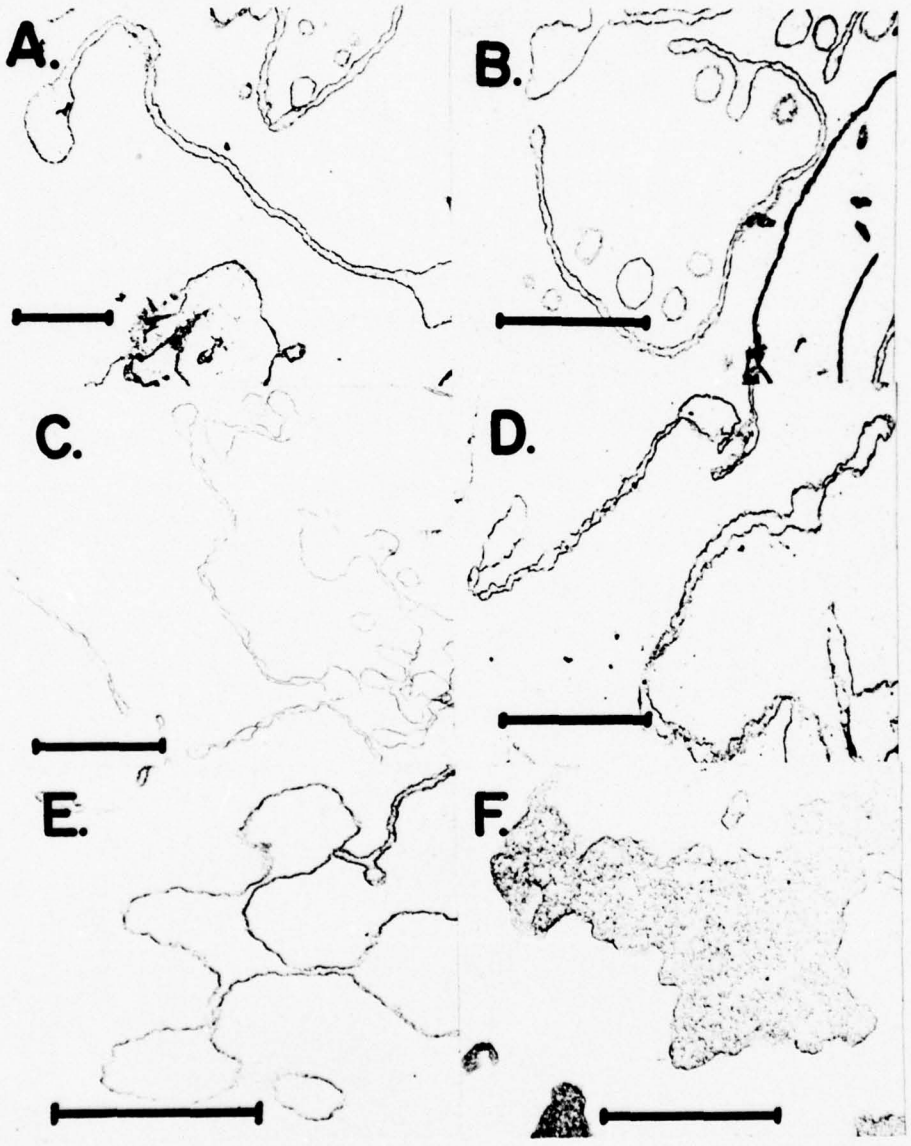

FIGURE 5

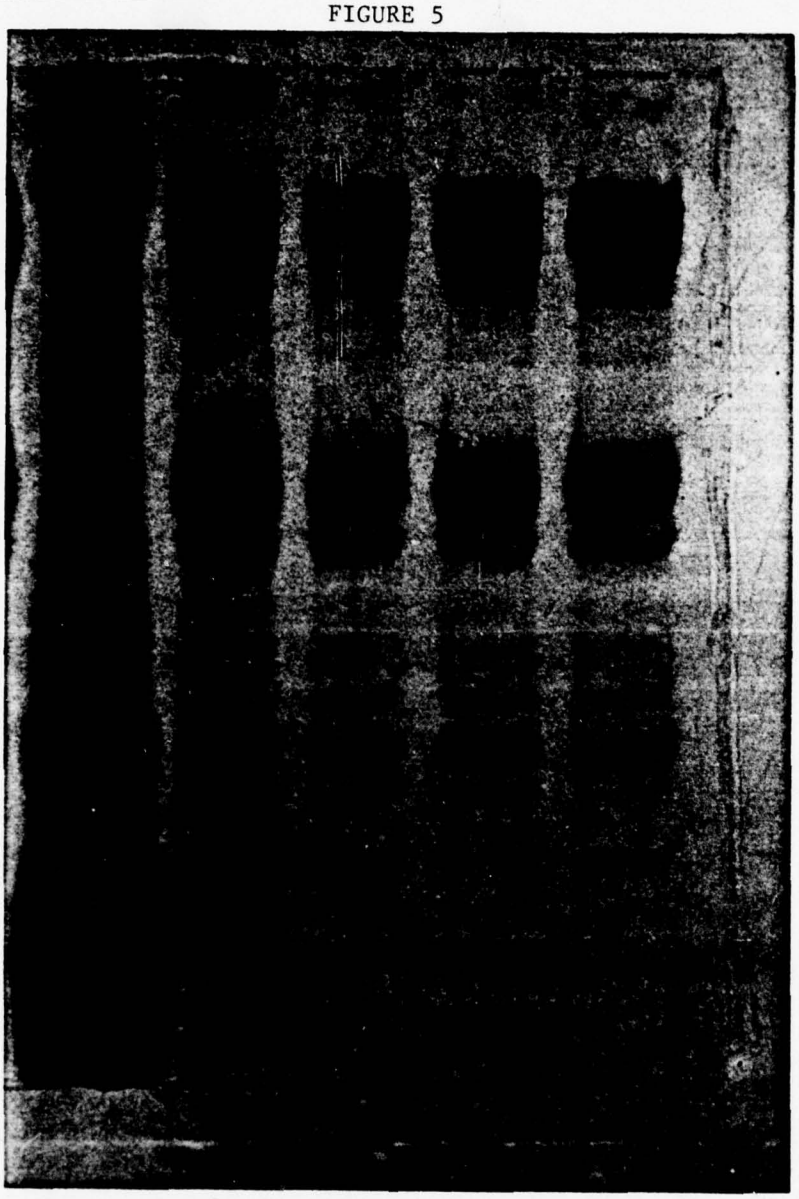

APPENDIX I

DERIVATION OF EQUATION FOR MEASURING ROTATIONAL CORRELATION TIME BY

BY

PHILIP D. MORSE, II

In a DC magnetic field, electrons precess around the field with a net magnetic moment parallel or antiparallel to the field.

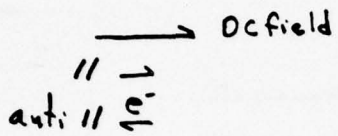

These two spin states represent different energy levels and transitions can be induced between these spin states by an oscillating magnetic (microwave) field at right angles to the DC field. The energy levels of the oscillating and static magnetic field must satisfy the equation

$$E = h\nu = g\beta H$$

where E = energy difference between spin states, h = Plank's constant, ν = frequency of the oscillating magnetic field, g = gyromagnetic ratio of the electron (2.0023 for a free electron), β = Bohr magneton, and H = DC magnetic field.

Other magnetic interactions occur in the sample, some time independent which we won't deal with much here, and some time dependent, which arise from molecular motion. The magnetic interactions are weak and the "pure" spin Hamiltonian is weakly coupled to the lattice Hamiltonian by the spin-lattice Hamiltonian. Thus, our information about molecular motion is not obtained directly from the spin alone.

Magnetic interactions between electron spins and the magnetic fields must take into account nuclear spins as well. This interaction gives rise to an energy contribution of $\mathcal{H}_I = a\vec{I}\cdot\vec{S}$ where a = isotropic hyperfine interaction constant. $\vec{I}$ is the nuclear spin and $\vec{S}$ is the electron spin.

If orbital angular momentum is incompletely quenched, the g and a values are anisotropic. Thus the Hamiltonian becomes

$$\mathcal{H} = \underline{\underline{g}}\beta\vec{H}\vec{S} + \underline{\underline{a}}\vec{I}\cdot\vec{S} \qquad 1)$$

where $\underline{\underline{g}}$ and $\underline{\underline{a}}$ are 2nd order tensors. We can separate this into an isotropic and anisotropic part

$$\mathcal{H}_{iso.} = g\beta\vec{H}\vec{S} + a\vec{I}\cdot\vec{S} \qquad 1a)$$

$$\mathcal{H}_{aniso} = (\beta)\underline{\underline{G}}\cdot\vec{S}\cdot\vec{H} + \vec{I}\cdot\underline{\underline{A}}\,\vec{S} \qquad 1b)$$

where $\underline{\underline{G}}$ and $\underline{\underline{A}}$ are traceless tensors and g and a are 1/3 (Tr g) and 1/3 (Tr a). $\underline{\underline{G}}$ and $\underline{\underline{A}}$ are equivalent to the anisotropic chemical shift and the anisotropic spin-spin interaction in NMR.

The total Hamiltonian is, finally

$$\mathcal{H} = \mathcal{H}_S + \mathcal{H}_L + \mathcal{H}_{SL} \qquad 2)$$

where $\mathcal{H}_S$ is a function only of nuclear and electron spin, $\mathcal{H}_L$ is a function only of intra and intermolecular nuclear co-ordinates, and $\mathcal{H}_{SL}$ is the spin lattice Hamiltonian which couples the spin system with the lattice.

In particular, we wish to solve for the magnetization (quantity actually measured during an experiment) which is given by

$$\vec{M}_{(t)} = \mathrm{Tr}\rho(t)g\cdot\vec{\underline{S}}\,(\mu/\hbar)(N/V) \qquad 3)$$

where $\vec{\underline{S}}$ is the electron spin operator, N/V is the spin density and $\mathrm{Tr}\rho(t)$ is the instantaneous density matrix over all spins.

To solve for the time evolution of $\rho(t)$ and $\vec{\underline{S}}(t)$, we use time-dependent perturbation theory where

$$\mathcal{H}_T = \mathcal{H}_1 + \lambda\mathcal{H}_2(t)$$

where $\lambda\mathcal{H}_2(t)$ is a small time-dependent perturbation.

The equations of motion for $\vec{\underline{S}}(t)$ and $\rho(t)$ are

$$\dot{\vec{\underline{S}}}(t) = i\left[\mathcal{H}_T(t),\ S(t)\right] \quad \text{and} \quad \dot{\rho}(t) = -i\left[\mathcal{H}_T(t),\ \rho(t)\right]$$

We expand $\vec{\underline{S}}(t)$ and $\rho(t)$ in powers of $\lambda\mathcal{H}_2$ assuming $\lambda\mathcal{H}_2$ has a slow time dependence.

For example, $\mathcal{H}_1$ will represent the Larmor precession of the electron about the DC

We obtain 4)

$$\vec{S}(t) = \vec{S}^{\circ}(t) + i\lambda \int_0^t dt' \left[\mathcal{H}^{\circ}_{SL}(t-t'), \vec{S}^{\circ}(t) \right] - \lambda^2 \int_0^{t'} dt'' \left[\mathcal{H}_{SL}(t-t'') \left[\mathcal{H}^{\circ}_{SL}(t-t'), \vec{S}^{\circ}(t) \right] \right]$$

ignoring higher orders of λ where $\vec{S}^{\circ}(t)$ is the precessing, non-relaxing spin and $\mathcal{H}^{\circ}_{SL}(t)$ is the time dependent portion of $\mathcal{H}_{SL}$. Similarly, if $\mathcal{H}_2$ is the external field

$$\rho(t) = \rho^{\circ}(t) + i\lambda(\mu^{\circ}/\hbar) \int_{t_0}^{t} dt' \left[S(t-t') \cdot g(t-t') \cdot b(t') \, \rho^{\circ}(t) \right] \qquad 5)$$

also ignoring higher orders of λ.

ESR experiments are continous wave experiments. The absorbed power is thus

$$P(t) = b_x' \cos \omega t \, \frac{dM_x(t)}{dt}$$

At small power levels b_x'

$$M_x(t) = \left[\chi'_{xx}(\omega) \cos \omega t + \chi''_{xx}(\omega) \sin \omega t \right] b_x' V$$

where V = volume. For one rf cycle

$\bar{P}(\omega) = \omega/2 \left(\chi''(\omega) \right) b_x' V$ where $\bar{P}(\omega)$ is the observed spectrum and $\chi''(\omega)$ is the representation of the line shape which is related to $M_x(t)$.

Since we cannot solve directly for $\rho(t)$ we substitute the perturbation expansions of this value into the magnetization equation

$$M_x(t) = g(\mu^{\circ}/\hbar) \, \mathrm{Tr} \, \rho(t) \, S_x \quad \text{to obtain}$$

$$M_x(t) = ig^2(\mu^{\circ}/\hbar)^2 \int_{-\infty}^{t} \mathrm{Tr} \left[S_x(\tau - t), \rho(eq) \right] S_x b_x' \cos \omega t$$

where $\mathrm{Tr} \, \rho(eq) \, S_x = 0$. We expand this to

$$M_x(t) = \int_{-\infty}^{t} d\tau \, \chi_{xx}(t-\tau) B_x' \cos \omega t$$

where

$$\chi''_{xx}(t-\tau) = ig^2(\mu^{\circ}/\hbar)^2 \langle S_x(t-\tau), S_x \rangle .$$

χ_{xx} can be broken down into χ'_{xx} and χ''_{xx} where $\chi''_{xx}(\omega) = \int_0^{\infty} d\tau \, \chi_{xx}(\tau) \sin \omega t$.

We can show that

$$\chi'_{xx}(\omega) = \frac{1}{kT} g^2 (\mu^{\circ}/\hbar)^2 \omega \int_0^{\infty} dt \, \langle S_x(t) S_x \rangle \cos \omega t$$

where $\langle \underline{S}_x(t)\underline{S}_x \rangle \to 0$ as $t \to \infty$.

$$\bar{P}(\omega) = \beta(g\mu_B/\hbar)^2(V/2)\omega^2 b_x'^2 \int_0^\infty dt \, \langle \underline{S}_x(t)\underline{S}_x \rangle \cos \omega t$$

To get an expression for the autocorrelation function $\langle S_x(t)S_x(0)\rangle$ we use the expansion for $S_x(t)$ to obtain

$$\langle \vec{\underline{S}}(t)\vec{\underline{S}}(0)\rangle = \langle \vec{\underline{S}}^\circ(t)\vec{\underline{S}}^\circ(0)\rangle - i\int_0^t dt' \langle \left[\mathcal{H}_{SL}(t-t'), \vec{\underline{S}}^\circ(t)\right]\vec{\underline{S}}(0)\rangle - \int_0^t dt \int_0^{t'} dt'' \langle \left[\mathcal{H}_{SL}(t-t'), \left[\mathcal{H}_{SL}(t-t''), \vec{\underline{S}}^\circ(t)\right]\right]\vec{\underline{S}}(0)\rangle + \ldots$$

where $\vec{\underline{S}}^\circ(t)$ is the simply precessing spin and

$$\mathcal{H}_{SL}(t) = e^{i(\mathcal{H}_S+\mathcal{H}_L)t}\,\mathcal{H}_{SL}\,e^{-i(\mathcal{H}_S+\mathcal{H}_L)t}.$$

All spin lattice terms can be written as $\mathcal{H}_{SL} = \sum_q \underline{F}_q^\circ \underline{S}_q^\circ$ where $\underline{F}_q^\circ$ and $\underline{S}_q^\circ$ are functions of the lattice and spin variables only, respectively. Thus (6)

$$\underline{F}_q^\circ(t) = e^{-i\mathcal{H}_L t}\,\underline{F}_q\,e^{-i\mathcal{H}_L t} \quad \text{and} \quad \underline{S}_q^\circ(t) = e^{i\mathcal{H}_S t}\,\underline{S}_q\,e^{-i\mathcal{H}_S t}$$

where $(^\circ)$ means that the time dependence is not derived from the complete Hamiltonian. $\langle \mathcal{H}_{SL}(t)\rangle = 0$ and $\langle \underline{F}_q^\circ(t)\rangle = 0$ at high enough temperature so the linear term in the autocorrelation function (linear in $\mathcal{H}_{SL}$) vanishes.

If we look at just the second order term

$$\langle \left[\mathcal{H}_{SL}(t-t'), \left[\mathcal{H}_{SL}(t-t''), \vec{\underline{S}}^\circ(t)\right]\right]\vec{\underline{S}}\rangle_0 = \sum_{q,q'} \langle F_q(t-t')F_{q'}(t-t'')\rangle \langle \left[\mathcal{S}_q(t-t'), \left[\mathcal{S}_q(t-t''), \vec{\underline{S}}^\circ(t)\right]\right]\vec{\underline{S}}(0)\rangle$$

where the averages over F use the lattice density matrix

$$\frac{e^{-\frac{\mathcal{H}_L}{kt}}}{\mathrm{Tr}\, e^{-\frac{\mathcal{H}_L}{kT}}}$$

and the averages over $\mathcal{S}$ involve the spin density matrix. Thus:

$$\langle \underline{F}_q^\circ(t-t')\underline{F}_q^\circ(t-t'')\rangle_0 = \langle \underline{F}_q^\circ(t''-t')\underline{F}_q^\circ\rangle_0$$

This involves only lattice dynamics; it is this parameter we wish to study.

Since we are interested only in terns in which $\left[\mathcal{H}_S, \mathcal{S}_q \mathcal{S}_{q'}\right] = 0$. and changing the variables of integration $T = t''+t'$ and $\tau = t''-t'$ we get

$$\langle \vec{\underline{S}}(t)\vec{\underline{S}}(0)\rangle = \langle \vec{\underline{S}}^\circ(t)\vec{\underline{S}}(0)\rangle_0 - \int_0^t d\tau\,(t-\tau) \sum_{q,q'} \langle \underline{F}_q \underline{F}_{q-q'}\rangle f(\tau) \langle \left[\mathcal{S}_{q'}(T), \left[\mathcal{S}_q, \vec{\underline{S}}^\circ(t)\right]\right]\vec{\underline{S}}\rangle_0 + \ldots$$

where $f(\tau)$, the "normalized" lattice correlation function, depends only

$$\langle F_q(\tau) F_{q'}(0)\rangle = \langle F_q F_{-q'}\rangle f_{q,q'}(\tau)$$

Assuming $f(\tau) \to 0$ for $t \to \infty$ and $\tau \gg \tau_c$ and $t \gg \tau_c$ where t is the spin relaxation term of interest, we finally get

$$\langle \vec{S}(t)\vec{S}(0)\rangle = \langle \vec{S}(t)\vec{S}(0)\rangle_o - \left(\sum_{q,q'} \langle F_q F_{q'}\rangle_o \int_0^\infty d\tau\, f_{q\,q'}(\tau) \langle [\mathcal{S}_q(\tau), [\mathcal{S}_{q'}, S(t)]]\, S\rangle_o\right) + \ldots$$

To evaluate $\vec{S}(t)$ we use

$$\langle a'|\, \vec{S}(t)\,|a''\rangle = \langle a'|\, \vec{S}\,|a''\rangle e^{i\omega_{a'a''}t}$$

where $|a\rangle$ is an eigenfunction of $\mathcal{H}_S$ and $\omega_{a'a''}$ is the Larmor frequency or

$$\omega_{a'a''} = \langle a'|\mathcal{H}_S|a'\rangle - \langle a''|\mathcal{H}_S|a''\rangle$$

where a' and a" represent the same nuclear spin state, but different electronic spin states. Finally,

$$\langle \vec{S}(t)\vec{S}(0)\rangle_o = \sum_{a'a''} e^{i\omega_{a'a''}t} \langle \vec{S}^{a'a''}\vec{S}\rangle_o$$

and

$$\langle [\mathcal{S}_q(\tau), [\mathcal{S}_{q'}, \vec{S}(t)]]\vec{S}\,_o\rangle = \sum_{a,b} e^{i\omega_{b'b''}\tau}\, e^{i\omega_{a'a''}t} \langle \mathcal{S}_q^{b'b''} [\mathcal{S}_{q'}^{a'a''}]]\, \vec{S}\rangle_o$$

or

$$\omega_{a'a''}\langle a'|\mathcal{H}_S|a'\rangle - \langle a''|\mathcal{H}_S|a''\rangle$$

becomes

$$\langle \vec{S}(t)\vec{S}(0)\rangle = \sum_{a'a''} e^{i\omega_{a'a''}t} \langle \vec{S}^{a'a''}\vec{S}\rangle_o \left\{1 - \sum_{b'b''} R_{a'a''b'b''}(\omega_{b'b''}) + \ldots\right\}$$

where the relaxation matrix $R_{a'a''b'b''}(\omega_{b'b''})$ is defined as

$$\sum_{qq'} \langle F_q F_{-q'}\rangle_o \langle \mathcal{S}_q^{b'b''} [\mathcal{S}_{q'}, S^{a'a''}]]\vec{S}\,\rangle_o \int_0^\infty d\tau\, f_{qq'}(\tau)\, e^{i\omega_{b'b''}\tau} \langle \vec{S}^{a'a''}\vec{S}\rangle_o$$

If we exponentiate:

$$\langle \vec{S}(t)\vec{S}(0)\rangle = \sum_{a'a''} e^{(i\omega_{a'a''} - \Delta\omega_{a'a''})t}\, e^{-t/T_{a'a''}} \langle \vec{S}^{a'a''}\vec{S}\rangle_o$$

where $T_{a'a''}$ is the relaxation time and $\Delta\omega_{a'a''}$ is a frequency shift where

$$T^{-1}_{a'a''} + i\Delta\omega_{a'a''} = \sum_b R_{a'a''b'b''}(\omega_{b'b''})$$

the relaxation matrix which are involved in the X direction (microwave direction) of the magnetization. Hence a'a" and b'b" must correspond to allowed ESR transitions. We must determine

$$\mathcal{H}_{SL} = (\mu/\hbar)\vec{H}\cdot\underline{\underline{G}}\,\vec{\underline{S}} + \vec{\underline{I}}\,\underline{\underline{A}}\,\vec{\underline{S}} \quad .$$

To do this, we define the shift operators

$$\underline{S}_{\pm} = \underline{S}_x \pm i\underline{S}_y$$

$$\underline{I}_{\pm} = \underline{I}_x \pm i\underline{I}_y \quad .$$

We obtain

$$\mathcal{H}_{SL} = \left[(\mu/\hbar)\, BG_{ZZ} + A_{ZZ}\underline{I}_Z\right]\underline{S}_Z + \qquad (a)$$

$$\left[A_{Z+}\underline{I}_+ + A_{Z-}\underline{I}_-\right]\underline{S}_Z \quad + \qquad (b)$$

$$\Big[(\mu_o/\hbar\ \ BG_{Z+} + A_{+Z}I_{-Z} + A_{++}\underline{I}_+ \qquad + A_{+-}\underline{I}_-)\underline{S}_- \ +$$

$$(\mu_o/\hbar)BG_{Z-} + A_{-Z}\underline{I}_Z + A_{--}\underline{I}_- + A_{-+}\underline{I}_+)\underline{S}_+\Big] \qquad (c)$$

where (a), (b), and (c) are the secular, pseudosecular, and nonsecular terms respectively.

We can write the terms for $\mathcal{H}_{SL}$ in the relaxation matrix for all three terms. Assuming that only one rotational diffusion constant is present, we describe the relaxation of a spin lattice term as

$$f_{qq'}(\tau) = \exp -\tau/\tau_c$$

and evaluate the static lattice correlation functions. We obtain

$$T_2^{-1}(I_Z) = \frac{1}{3}\ \frac{4}{5}\left(\frac{\Delta g^2}{3} + \delta g^2\right)(\mu/\hbar)^2H^2 + \frac{1}{10}\left(\Delta a^2 + 3\delta a^2\right)I(I+1) + \frac{1}{6}\left(\Delta a^2 + 3\delta a^2\right)I_Z$$

$$+ \frac{8}{15}\left(\Delta a\Delta g + 3\delta g\ \delta a\right)(\mu/\hbar)HI_Z\,\tau_c + \frac{1}{5}\left(\frac{\Delta g^2}{3} + \delta g^2\right)(\mu/\hbar)H^2$$

$$+ \frac{7}{18}\left(\Delta a^2 + 3\delta a^2\right)I(I+1) - \frac{1}{18}\left(\Delta a^2 + 3\delta a^2\right)I_Z{}^2 + \frac{2}{3}\left(\Delta g\Delta a + 3\delta g\ \delta a\right)(\mu/\hbar)BI_Z\,\frac{\tau_c}{1+\gamma^2B^2\tau_c^2}$$

where $\Delta a = a_{zz} - \frac{1}{2}(a_{xx}-a_{yy})$, $\delta a = \frac{1}{2}(a_{xx}-a_{yy})$, $\Delta g = g_{zz} - \frac{1}{2}(g_{xx}-g_{yy})$, and $\delta g = \frac{1}{2}(g_{xx}-g_{yy})$.

If we assume axial symmetry of the g and a tensors, as is found in nitroxides, and factor out unnecessary terms, we finally arive at the equation:

$$T_2^{-1}(I_Z) = \left\{ \left[3I(I+1) + 5I_Z^2\right] \frac{b^2}{40} + \frac{4}{45} (\Delta\gamma H)^2 - \frac{4}{15} b\Delta\gamma H I_Z \right\} + X \qquad 8)$$

where T_2^{-1} is the spin-spin relaxation time, I_Z is the nuclear spin state, I is the nuclear quantum spin number, b is $4/3\pi(a_{zz} - \frac{1}{2}(a_{xx}+a_{yy}))$ and $\Delta\gamma$ is $-|\beta|/h\ (g_{zz} - \frac{1}{2}(g_{xx}+g_{yy}))$. X = unknown additional magnetic contributions.

When we rearrange this to powers of I_Z we get

$$T_2^{-1}(I_Z) = A + BI_Z + CI_Z^2 \quad \text{where } \frac{B}{\tau_c} = \frac{4}{15} b\Delta\gamma H \text{ and } \frac{C}{\tau_c} = \frac{5b^2}{40}$$

where all calculations of g and a are in cycles per second. It is thus apparent that, relative to the central line (I_Z=0), the I_Z = (1) line will be broader, and the I_Z = (-1) line will be broader yet. We will see that this in fact happens with the nitroxide ESR spectra.

In order to calculate correlation time, we rearrange the above equation using the substitution $T_{2(0)}^{-1} = 4/45(\Delta\gamma H)^2$ to:

$$\left[\frac{T_{2(0)}}{T_{2(I_Z)}} - 1\right]\left[\frac{\pi\sqrt{3\Delta\omega}}{b}\right] - \left[\frac{4\Delta\gamma H(I_Z)}{15} + \frac{1}{8} b(I_Z)^2\right]^{-1} = \tau_c \qquad 9)$$

When we substitute in values for b, $\Delta\gamma$, H (approximately 3400 gauss), I_Z = -1 we obtain the equation:

$$\tau_c = 6.5 \times 10^{-10}\left[\left(\frac{h_o}{h_{-1}}\right)^{\frac{1}{2}} - 1\ W_0\right] \qquad 10)$$

where h_0 = midfield line height, h_{-1} = high field line height, and W_0 = midfield linewidth. We substitute line widths for relaxation times $T_{2(I_Z)}^{-1} = \pi\sqrt{3\Delta\omega}$ where $\Delta\omega$ is the first derivative linewidth in cycles per second (2.8×10^6 cps = 1 gauss) and, since the line heights are related to the line widths by the equation $A=w^2h$, we substitute $\left(\frac{h_o}{h_{-1}}\right)^{\frac{1}{2}}$ for $\frac{T_{2(0)}}{T_{2(-1)}}$. It is this equation that we use to calculate rotational correlation time. Limitations in this equation will be discussed in the seminar.

REFERENCES

Kivelson, D. (1960) J. Chem. Phys. 33:1094.

Kivelson, D. (1971) in "Electron Spin Relaxation in Liquids", L.T. Muus and P.W. Atkins, Eds. Plenum Press, New York. Pages 213-273.

Kubo, R. and Tomita, K. (1959) J. Phys. Soc. Japan 9:888.

McConnell, H.M. (1956) J. Chem. Phys. 25:709.

Nordio, P.L. (1976) in "Spin Labeling Theory and Applications", L.J. Berliner, Ed. Academic Press, New York, Pages 5-52.

Stone, T., Buckman, T., Nordio, P., and McConnell, H.M. (1965) Proc. Natl. Acad. Sci. U.S. 54:1010.

TYPICAL VALUES FOR g AND HYPERFINE CONSTANTS FOR SOME SPIN LABELS

	g_{xx}	g_{yy}	g_{zz}	a_{xx}	a_{yy}	a_{zz}
TEMPONE	2.0104	2.0074	2.0026	5.2	5.2	31
TEMPO	2.0103	2.0069	2.0030	-	-	-
5NS	2.0088	2.0061	2.0027	6.3	5.8	33.6

TEMPONE

TEMPO

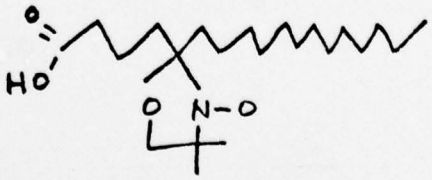

5NS

APPENDIX II

Chemistry and Physics of Lipids 20 (1977) 295–303

LOCALIZATION OF THE MEMBRANE PERTURBER ADAMANTYL SULFATE IN SARCOPLASMIC RETICULAR VESICLES

Philip D. MORSE, II*

Department of Biochemistry and Biophysics, The Pennsylvania State University, University Park, Pa. 16802 USA

Received May 17th, 1977 accepted June 27th, 1977

The properties of a new membrane perturbing agent, adamantyl sulfate (A-1-S) are described. Lobster sarcoplasmic reticular vesicles (SRV) were used as a test membrane system and the activity of the Ca^{2+} – Mg^{2+}-dependent ATPase in conjunction with spin label data was used to determine the location of A-1-S in the membrane. The results suggest that A-1-S perturbs only the polar region of the SRV and that this causes loss of ATPase function. Thus, ATPase activity requires integrity of the membrane polar region.

I. Introduction

The Ca^{2+}–Mg^{2+}-dependent ATPase of sarcoplasmic reticulum (SR) is a lipid requiring enzyme which appears to be located in the outer half of the SR membrane [1]. Reconstitution experiments using the purified enzyme in artificial phospholipid systems have shown that the enzyme requires a hydrocarbon region for activity [2,3], but the requirements of the enzyme for the phospholipid polar group are less clear. One laboratory has shown that phosphatidyl choline (PC) alone will reactivate the purified SR ATPase [2,3], while another has shown that both PC and phosphatidyl ethanolamine (PE) are required [4]. Removal of the phospholipid head group by phospholipase C inactivates the enzyme [5].

The role of the phospholipid head groups in maintaining activity of the SR ATPase is not well understood, but one possible function is that of maintaining a certain spacing or change density around the enzyme. Such a hypothesis could be tested in a naturally occurring membrane system by perturbing the packing of lipids in the polar region of the membrane without affecting the hydrocarbon region. A selective perturbing agent for this purpose can be derived from the cage hydrocarbon adamantane, which has been shown to be an effective perturber of the membrane in a variety of artificial and natural membranes [6–8].

This paper describes spin label and enzyme assay experiments which demonstrate that adamantyl sulfate (A-1-S) effectively perturbs only the polar region of both model

* Present address: Department of Biology, Wayne State University, Detroit, Mich. 48202, U.S.A.

membrane systems and SRV. The data show that disturbing the packing of phospholipids in the polar region of the SR membrane reduced the ATPase activity and this suggests that the density of phospholipids head groups in the SR membrane is important in maintaining ATPase activity.

II. Materials and Methods

A. Sarcoplasmic reticular vesicles

SRV was obtained from lobster abdominal muscle by the method of Deamer [9] and stored at 2°C at 16 mg protein/ml for not longer than 3 days.

B. Perturbing agents

A perturbing agent specific for the polar region of the membrane was derived from adamantane. Adamantyl sulfate (A-1-S) was synthesized from adamantane carboxylic acid by reacting with chlorosulfonic acid. The product was stored in water at 20 mM or 200 mM. A-1-S was generously provided by Dr. A.D. Keith.

C. Sulfate assay

Membrane-bound A-1-S was measured by a modification of the sulfate assay of Spencer [10]. Aliquots of SRV treated with A-1-S were spun down at 40,000 *g* for 30 min, and the total sulfate of the supernatant was measured. The supernatants, containing about 0.1 to 0.2 μM of sulfur, were dried; 0.2 ml of 30% nitric acid was added; this was boiled to dryness. After cooling 0.4 ml of ethanol was added to each tube, followed by 0.1 ml of 0.5 M acetate buffer (pH 4) containing 36.25 μg of K_2SO_4 and 10 mg of barium chloranilate per ml. The solution was repeatedly mixed with a vortexer for 10 minutes and centrifuged at 1,000 *g* for 1–2 min. An aliquot of the supernatant (0.2 ml) was diluted to 2.00 ml and the optical density measured at 327.5 nM on a Beckman DB spectrophotometer. K_2SO_4 was used as a standard and 0.25 μmol of sulfate gave an absorbance of 0.96. Typically, 70% of the A-1-S added was found in the supernatant, consequently, all data obtained in the presence of A-1-S is corrected for this and reflects only the effects of membrane-bound A-1-S.

D. Addition of perturbers to SRV and multilamellar vesicles

A quantity of A-1-S corresponding to a final molecular ratio of one spin label per 50 SRV phospholipids up to two spin labels per SRV phospholipid was added to small test tubes, dried, the SRV added and mixed with a vortexer for several minutes. Sulfate assays were made to determine the amount of A-1-S incorporated into the membrane. 25 μl of this membrane A-1-S mixture was used for measurements of calcium uptake

and ATP hydrolysis. No decrease in light scattering of the SRV was observed at any A-1-S concentration.

E. Calcium uptake and ATPase assay

This assay is essentially that described by Deamer [9]. 2.4 ml of the reaction buffer (1 mM TES–NaOH buffer, pH 7.3, 5 mM $MgCl_2$, 4 mM potassium oxalate and 2 mM ATP) were placed in a 5 ml beaker with a pH electrode and magnetic stirring bar. 25 μl of SRV (corresponding to 0.4 mg protein) were added and the reaction started with 0.5 μmol of calcium chloride. The hydrolysis of ATP and release of hydrogen ions associated with calcium uptake was measured by a Metrohm pH meter and recorded on a Varian chart recorder. When all the calcium was taken up, the reaction stopped and the solution was then back-titrated with a calibrated solution of KOH to determine the amount of hydrogen ions generated. 50 μl of 2% Triton X-100 was then added to uncouple calcium transport from ATP hydrolysis. The initial rate of the uncoupled reaction gave the ATPase rate. Normal SRV has a calcium pumping rate of 0.59 ± 0.12 μM $Ca^{2+} \cdot min^{-1} \cdot mg^{-1}$ protein and ATPase rates of 0.94 ± 0.21 μM $ATP \cdot min^{-1} \cdot mg^{-1}$ protein. The control Ca^{2+}/H^+ ratio was 1.68 ± 0.72. This value was seasonally dependent and was as low as 1.0 in lobsters obtained in the winter. In untreated SRV, calcium uptake, as measured by the pH decrease, proceeds linearly and stops after 45–60 s when calcium in the medium is exhausted.

Disruption of the SRV membrane leads to uncoupling of calcium transport and ATP hydrolysis and is observed experimentally as a curvilinear decrease in pH. The three parameters to be measured are: (1) calcium ions pumped per hydrogen ion generated (per ATP hydrolysed). (Maximum coupling is indicated by a ratio of 2.0, while smaller ratios would indicate disruption of membrane structure); (2) rate of calcium uptake (smaller values would indicate enzyme inhibition); (3) ATPase rate (a decrease in the rate of calcium uptake with no change in the Ca^{2+}/H^+ ratio with no decrease in calcium uptake or ATPase activity would indicate disruption of membrane structure alone.)

F. Spin labeling

The spin label 2N14 was a gift from Dr. Alec D. Keith. 7N14 was prepared by reacting MgBr-heptane with heptanoyl chloride. The product, 7 keto tetradecane, was distilled under vacuum and the oxazolidine-N-oxyl prepared by the method of Keana et al. [11] The detailed synthesis and purification of 7N14 will be described later (Morse, Lusczakoski and Kavieff, to be published). All spin labels were stored in the cold in ethanol at concentrations of 20 mM.

Correlation time [12] was obtained from the first derivative spectra by the equation:

$$\tau_c = K W_0 \left\{ \left(\frac{h_0}{h_{-1}} \right)^{\frac{1}{2}} - 1 \right\}$$

where K = (6.5×10^{-10}), τ_c = correlation time, W_0 = width of the midfield spectral line, h_0 = height of the midfield spectral line, and h_{-1} = height of the high field spectral line. For Arrhenius plots of τ_c vs. temperature, the spin labels were added to the SRV or DPL vesicles at concentrations of one spin per 50 phospholipids. For the SRV, this was done by first adding the spin label in ethanol to a 6 X 50 mm test tube, evaporating the ethanol with nitrogen, adding the SRV, and vortexing for several minutes. For artificial dipalmitoyl lecithin (DPL) vesicles, spin labels were added directly to the DPL in chloroform at ratios of one spin label per 50 phospholipids and the vesicles were then prepared by the method of Johnson et al. [13]. ESR spectra were taken on a Varian 4500 or a Varian E-109E with temperature control accurate to 0.1°C.

III. Results.

A. Effect of A-1-S on ESR spectra from spin labeled DPL vesicles and SRV

It was first necessary to determine the locus of perturbation of A-1-S in artificial phospholipid vesicles and in the SRV. This could be accomplished by using spin labels

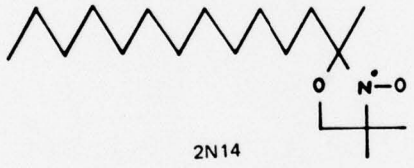

2N14

which are known to probe certain regions of the membrane. 2N14 probes the part of the membrane close to the polar region while 7N14 probes the hydrophobic interior [14]. Figure 1 shows an Arrhenius plot of τ_c versus 1/T for each of these spin labels in

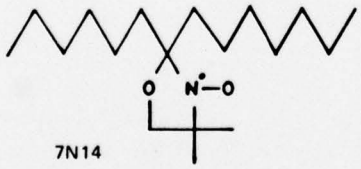

7N14

DPL vesicles with or without A-1-S. When A-1-S is present, the hydrophobic region of the membrane is clearly unaffected, but the polar region shows an increase in fluidity and a loss of the characteristic phase transition of DPL at 41°C. In SRV labeled with 2N14, a fluidity increase and loss of phase transition at 16°C is also observed (fig. 2). This indicates that A-1-S perturbs the artificial vesicles and SRV membrane in the polar region.

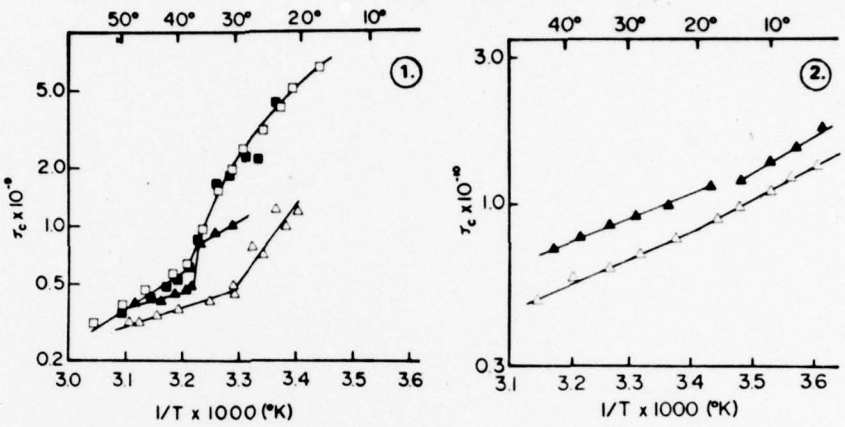

Fig. 1. Rotational correlation time at a function of temperature for the spin labels 2N14 (△) and 7N14 (□) in dipalmitoyl lecithin multilayers. Rotational correlation time (τ_c) was measured as described in the text. The solid figures represent dipalmitoyl lecithin in the absence of adamantyl sulfate while the open figures represent diplamitoyl lecithin in the presence of adamantyl sulfate at ratios of 5 lipids per adamantyl sulfate. A distinct 'melt' is observed for dipalmitoyl lecithin around 41°C in the absence of adamantyl sulfate. This melt is indicated by changes in τ_c for both spin labels. When adamantyl sulfate is present, τ_c for 7N14 is unaffected, but τ_c changes for 2N14. The region monitored by 2N14 becomes more fluid and the former transition at 41°C is shifted downward to below 30°C.

Fig. 2. Rotational correlation time as a function of temperature for the spin label 2N14 in sarcoplasmic reticular vesicles. Solid figures represent sarcoplasmic reticular vesicles in the absence of adamantyl sulfate. Under these conditions, a 'phase transition' is observed at 17°C. When adamantyl sulfate is present (open figures), the vesicles become more fluid and the transition at 17°C disappears.

B. Effect of A-1-S and detergents on SRV ATPase and calcium transport.

A-1-S

A-1-S is very effective in disrupting the ATPase and calcium transport properties of SRV. Figure 3 plots the ratio of perturbing molecules per SRV phospholipid against

the Ca^{2+}/H^{+} ration, Ca^{2+} uptake and ATPase activity. A-1-S causes complete uncoupling of calcium transport and ATP hydrolysis at ratios of one molecule of membrane bound A-1-S per 20 SRV phospholipids. A-1-S also inhibited Ca^{2+} uptake and the activity of the uncoupled ATPase at similar concentrations.

The experiments were repeated with a sulfate containing detergent, sodium dodecyl sulfate (SDS) to be certain that loss of ATPase activity was not due to the sulfate group on A-1-S. Unlike A-1-S, however, SDS solubilized the SRV membrane at high concentrations. A typical experiment is shown in table 1. As expected, SDS effectively uncoupled Ca^{+} transport and ATPase activity at ratios of 1 SDS per 5 SRV phospholipids. The ATPase rate increased at this concentration of SDS in the SRV membrane, but at higher concentrations, SDS reduced ATPase activity.

IV. Discussion

This report has attempted to show that A-1-S exerts its effect on the SR ATPase by disruption of the packing of the membrane phospholipids in the polar region. The decrease in the Ca^{2+}/H^{+} ratio with increasing A-1-S concentration suggest that the membrane structure sufficiently altered so that Ca^{2+} can leak out of the vesicles. This is not surprising; a number of detergents can do this as well. What is surprising is that this effect is observed solely by perturbations which are localized in the polar region of the membrane and are not transmitted to the hydrocarbon region. This is substantiated by the spin label data.

A. Enzyme data

The data obtained for the effect of A-1-S on the SRV membrane and ATPase suggest that the action of A-1-S on the ATPase is through its effect on the membrane and not through direct interaction with the ATPase itself. It is apparently

Table 1

Effect of SDS on the functions of SRV ATPase. All values are as percent of control. Membranes were prepared as in fig. 1. SDS rapidly uncoupled the membrane at concentrations above one molecule per 50 membrane phospholipids (1 : 50). Higher concentrations (1 : 5) of SDS caused an activation of Ca^{2+}, transport but at ratios of 1 : 0.5 Ca^{2+}, transport was inhibited. A similar result is obtained for the ATPase.

SDS : phospholipid ratio (%)	Ca^{2+}/H^{+} ratio	ATPase	Ca^{2+} uptake
1 : 50 (0.01%)	83	58	92
1 : 5 (0.1%)	0	137	155
1 : 0.5 (1.0%)	0	28	63

fortuitous that A-1-S causes a decrease in Ca^{2+}/H^{+} ratios and an ATPase rate decrease at about the same concentration. This similarity is not observed when the SRV are treated with SDS, which is a much more effective uncoupler of the ATPase and decreases Ca^{2+}/H^{+} ratios to zero at about 1/10 the concentration required for a similar effect by A-1-S. This further suggests that calcium permeability of the SRV membrane is more likely related to the integrity of the membrane hydrocarbon region.

B. Effect of detergents on the SR ATPase

SDS acts on the SRV membrane by essentially solubilizing it and this is demonstrated by a loss of turbidity of the SRV at higher SDS concentrations (2 SDS molecules per SRV phospholipids). At this concentration, enzyme activity is lost but at lower

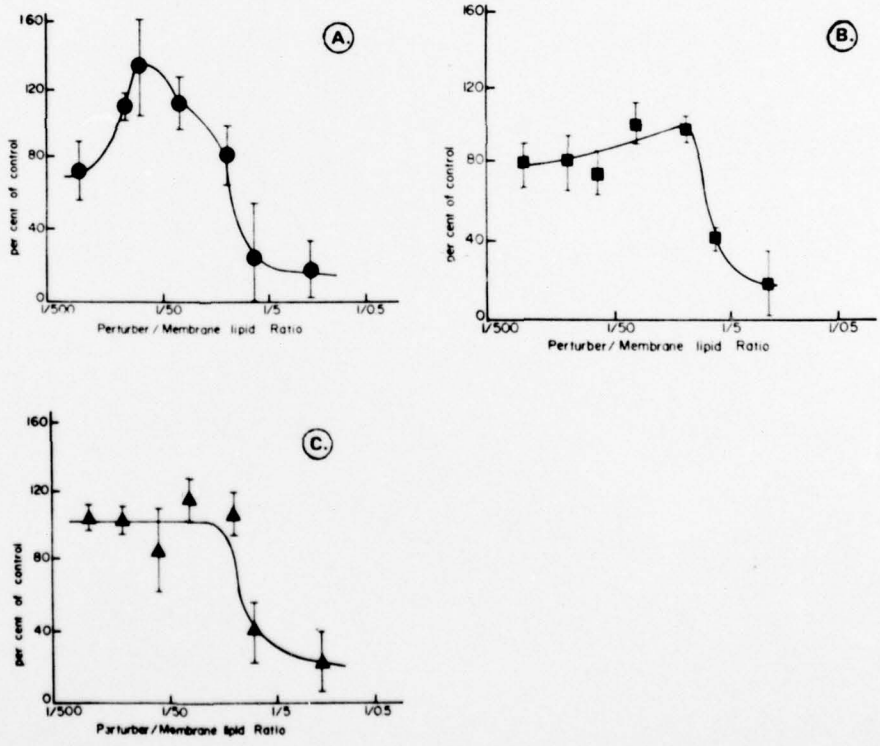

Fig. 3. Effects of adamantyl sulfate on the calcium-magnesium-dependent ATPase of sarcoplasmic reticular vesicles. Membrane phospholipid: adamantyl sulfate ratios are plotted against (A) Ca^{2+}/H^{+} ratios, (B) Ca^{2+} uptake and (C) ATPase activity. Experimental details are in the text.

concentrations, SDS activates the ATPase. This activation arises by uncoupling ATP hydrolysis from transport of calcium into the SRV. Under these conditions, the enzyme is essentially 'free running', and activities of the ATPase can be 2–3 times as great as when it is transporting calcium [9].

In contrast to SDS, A-1-S does not visually affect SRV turbidity and does not cause activation of the enzyme even though enzyme activity is uncoupled from calcium transport (fig. 3). This indicates that A-1-S does not solubilize the SRV and that the membrane remains essentially intact on a gross level. The A-1-S molecules apparently exert their effects as impurities and not as gross disruptors of membrane structure.

C. ESR Data

The ESR parameter rotational correlation time, τ_c, has a definite meaning in physical terms. Its derivation depends upon knowledge of the hyperfine and g-values derived from ESR studies of the spin label in a crystal form. The spin labels used in this study have not been analyzed in this manner, so, the τ_c measurements should not be interpreted as absolute number, however, these values are very useful for comparing the motion of spin labels located in different parts of the membrane, and in this sense, do provide meaningful data.

The data obtained from the spin label 2N14 shows that A-1-S clearly increases only in the polar region. Evidence is strong that 2N14 membrane fluidity indeed monitors the membrane polar region [14]; it also shows some partitioning into the aqueous phase below the transition temperature of the DPL vesicles. In contrast the precise location of 7N14 in the membrane hydrocarbon region is unknown. It does not distribute randomly within the hydrocarbon region [14] and is probably sampling a region of the membrane about half-way along the phospholipid chain. The depth to which A-1-S affects the SRV membrane cannot be precisely determined using 7N14, however, the limit of the perturbing effect of A-1-S is probably within 4–5 carbon atoms of the phospholipid head group.

Acknowledgements

Part of this work was performed as a post-doctoral student in the laboratory of Dr. A.D. Keith. Support was obtained from ERDA contract AT (11-1) 2223 to ADK and from ONR contact (N00014-76-C1167) to myself. I wish to thank Kenneth G. Pote for excellent technical assistance in obtaining the ESR spectra of the DPL vesicles and the Post House Tavern, State College, Pa., which made a gift of the lobsters used in this study.

References

[1] N. Yamanaka and D.W. Deamer, Biochim. Biophys. Acta 426 (1976) 132
[2] G.B. Warren, P.A. Poon, N.J. Birdsall, A.G. Lee and J.L. Metcalfe, Proc. Natl. Acad. Sci. USA 71 (1974) 622

[3] G.B. Warren J.C. Metcalfe, A.G. Lee, and N.J.M. Birdsall, FEBS Lett. 50 (1975) 261
[4] A.F. Knowles, E. Eytan and E. Racker, J. Biol. Chem. 251 (1976) 5161
[5] A. Martinosi, J. Donley and R.A. Halpin, J. Biol. Chem. 243 (1968) 61
[6] S. Eletr, M.A. Williams, T. Watkins and A.D. Keith, Biochim. Biophys. Acta. 339 (1974) 190
[7] J. Cupp, M. Klymkowski, J. Sands, A. Keith and W. Snipes, Biochim. Biophys. Acta 389 (1975) 345
[8] M.K. Jain, N. Yen-Min Wu, T.K. Morgan, M.S. Briggs and R.K. Murray, Chem. Phys. Lipids 17 (1976) 71
[9] D.W. Deamer, J. Biol. Chem. 248 (1973) 5477
[10] B.C. Spencer, Biochem. J. 75 (1970) 435
[11] J.F. Keana, S.B. Keana and D. Beetham, J. Am. Chem. Soc. 89 (1967) 3055
[12] A. Keith, F. Bulfield and W. Snipes, Biophys. J. 10 (1970) 618
[13] S.M. Johnson, A.D. Bangham, M.W. Hill and E.D. Korn, Biochim. Biophys. Acta 233 (1971) 820
[14] P.D. Morse II, M. Ruhlig, W. Snipes and A.D. Keith, Arch. Biochem. Biophys. 168 (1975) 40